Interim report of project TOKEDGE

A BOUT++ extension for interplay between flow, low-n mode and turbulence

Haruki Seto (QST)

Project Title: Collaboration on code development and simulations of tokamak edge MHD and turbulence (FY2020-FY2021, 2 years)

Outline

- Introduction: BOUT++ code and objectives of TOKEDGE project
- Numerical Issue on Poisson solvers in BOUT++ and a new 2D Poisson solver for low-n modes
- Verification test of 2D Poisson solver by linear problems (pressure-driven modes)
- Preliminary pedestal collapse simulation in annular full tours domain in shifted circular geometry
- Summary and future work (research plan in FY2021)

BOUT++ code and objectives of TOKEDGE project

BOUT++ framework as an edge tokamak simulation code [Dudson CPC2009]

- BOUT++ calculates middle-n (O(n)>1) and high-n (O(n)≫1) structure with high accuracy in complex boundary region in tokamak plasmas

- BOUT++ employs flute-ordering $k_{//}=0$ on Poisson solver for n≠0 modes calculating flow potential from vorticity

  ✓ Flute-ordering may not be accurate for low-n modes (O(n)~1) especially in diverted geometries

TOKEDGE is a two years project to extend BOUT++ framework for tokamak edge simulation solving interplay between n=0, low-n, middle-n and high-n modes in diverted geometries

➡ improvement of current-driven ELMs, RMPs, full annular tours edge turbulence simulations, etc…

- FY2020: development of flute-ordering-free Poisson solver for low-n modes (main topic of this talk)

Outline

- Introduction: BOUT++ code and objectives of TOKEDGE project
- Numerical Issue on Poisson solvers in BOUT++ and a new Poisson solver developed for low-n modes
- Verification test of 2D Poisson solver by linear problems
- Preliminary pedestal collapse simulation in annular full tours domain in shifted circular geometry
- Summary and future work (research plan in FY2021)

Numerical issue on Poisson solver in BOUT++ : flute ordering on low-n modes

BOUT++ describes differential operators with radial (ψ) derivative of flux surface coords. (ψ, θ, ζ) and parallel (y) derivative of field-aligned coords. (x, y, z) a.k.a. shifted metric and radial derivative method

Linearized Poisson solver for $n=n'$ mode vorticity ($n_{i1}/n_{i0} \ll O(1)$) in Fourier space

$$U_1(\cdot,\cdot,n') = \nabla\cdot\left(\frac{n_{i0}}{B_0}\nabla_\perp\phi_1\right) = \mathcal{L}_{\rm shifted}(\partial_\psi, \partial_\psi^2, \partial_y, \partial_y^2, n)\phi_1(\cdot,\cdot,n') \longrightarrow \phi_1(\cdot,\cdot,n') = \mathcal{L}^{-1}_{\rm shifted}(\partial_\psi, \partial_\psi^2, \partial_y, \partial_y^2, n')U_1(\cdot,\cdot,n') \quad ?$$

Poisson solver however cannot be defined as a boundary problem straightforwardly due to coexistence of ψ-derivatives (flux-surface coords.) and y-derivatives (field-aligned coords.)

- 1D Poisson solver in flux-surface coordinates for $n\neq0$ modes using flute-ordering approximation ($\partial_y=0$) [Dudson CPC2009]

$$\phi_1(\psi,\theta,n') = \mathcal{L}^{-1}_{\rm shifted}(\partial_\psi, \partial_\psi^2, n')U_1(\psi,\theta,n')$$

- 2D Poisson solver in field-aligned coordinates for $n=0$ mode using toroidal symmetry ($\partial_x=\partial_\psi+I\partial_\zeta=\partial_\psi$) [Dudson PPCF2017]

$$\phi_1(x,y) = \mathcal{L}^{-1}_{\rm shifted}(\partial_x, \partial_x^2, \partial_y, \partial_y^2)U_1(x,y)$$

Flute-ordering-free 2D Poisson solver for low-n modes is developed

- 2D Poisson solver in flux-surface coordinates for low-n modes with flux-surface coordinates' metrics

$$\phi_1(\psi,\theta,n') = \mathcal{L}^{-1}_{\mathrm{flux\ surface}}(\partial_\psi, \partial^2_\psi, \partial_\theta, \partial^2_\theta, n')U_1(\psi,\theta,n')$$

  - Self-consistent flow potential without flute-ordering for low-n modes
  - Poloidal grid resolution must be fine enough to describe poloidal structure of low-n modes
  - Iterative solver (PETSc library+ hypre* preconditioning) based on Ref.[Dudson PPCF 2017]
  - Applicable for non-diverted geometry (circular), single-null and double-null diverted geometries

Workflow in Poisson solver function developed in TOKEDGE

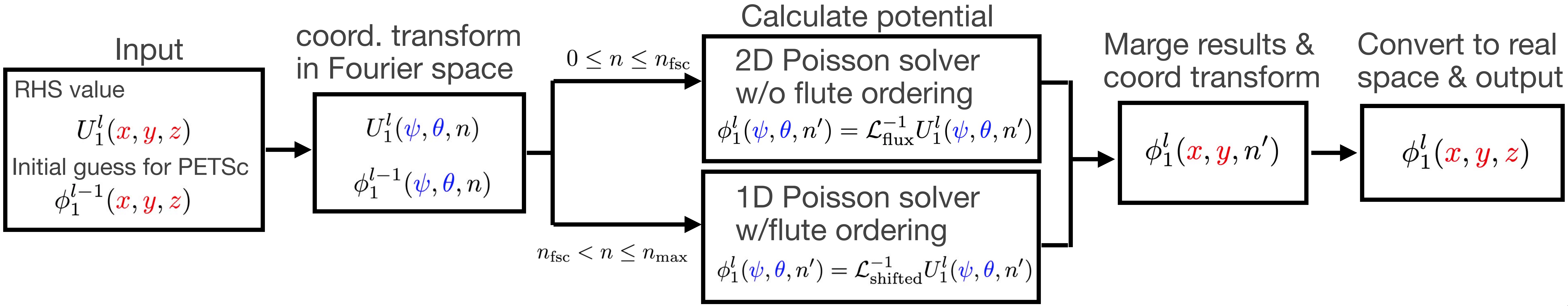

[*] hypre webpage: https://computing.llnl.gov/projects/hypre-scalable-linear-solvers-multigrid-methods

Outline

- Introduction: BOUT++ code and objectives of TOKEDGE project
- Numerical Issue on Poisson solvers in BOUT++ and a new 2D Poisson solver for low-n modes
- Verification test of 2D Poisson solver by linear problems (pressure-driven modes)
  - Ideal ballooning mode instability in shifted circular geometry
  - Resistive ballooning mode instability in single-null diverted geometry
- Preliminary pedestal collapse simulation in annular full tours domain in shifted circular geometry
- Summary and future work

2D Poisson solver is tested by comparing linear IBM growth rate in circular geometry by 2D Poisson solver and 1D flute-ordered Poisson solver

Linearized IBM model

$$\frac{\partial \varpi_1}{\partial t} = B_0 \partial_\parallel \left(\frac{J_\parallel}{B_0}\right) - B_0 \left[A_{1\parallel}, \frac{J_{\parallel 0}}{B_0}\right] + \frac{\boldsymbol{b}_0 \times \boldsymbol{\kappa}_0 \cdot \nabla P_1}{B_0}$$

$$\frac{\partial P_1}{\partial t} = -\left[\phi_1, P_0\right]$$

$$\frac{\partial A_{\parallel 1}}{\partial t} = -\partial_\parallel \phi_1$$

$$\varpi_1 = \nabla \cdot \left(\frac{1}{B_0^2} \nabla_\perp \phi_1\right), \quad J_{\parallel 1} = \nabla_\perp^2 A_{\parallel 1}$$

- constant ion density $n_{i0} = 10^{19}$ [m-3]
- normalized with poloidal Alfven unit

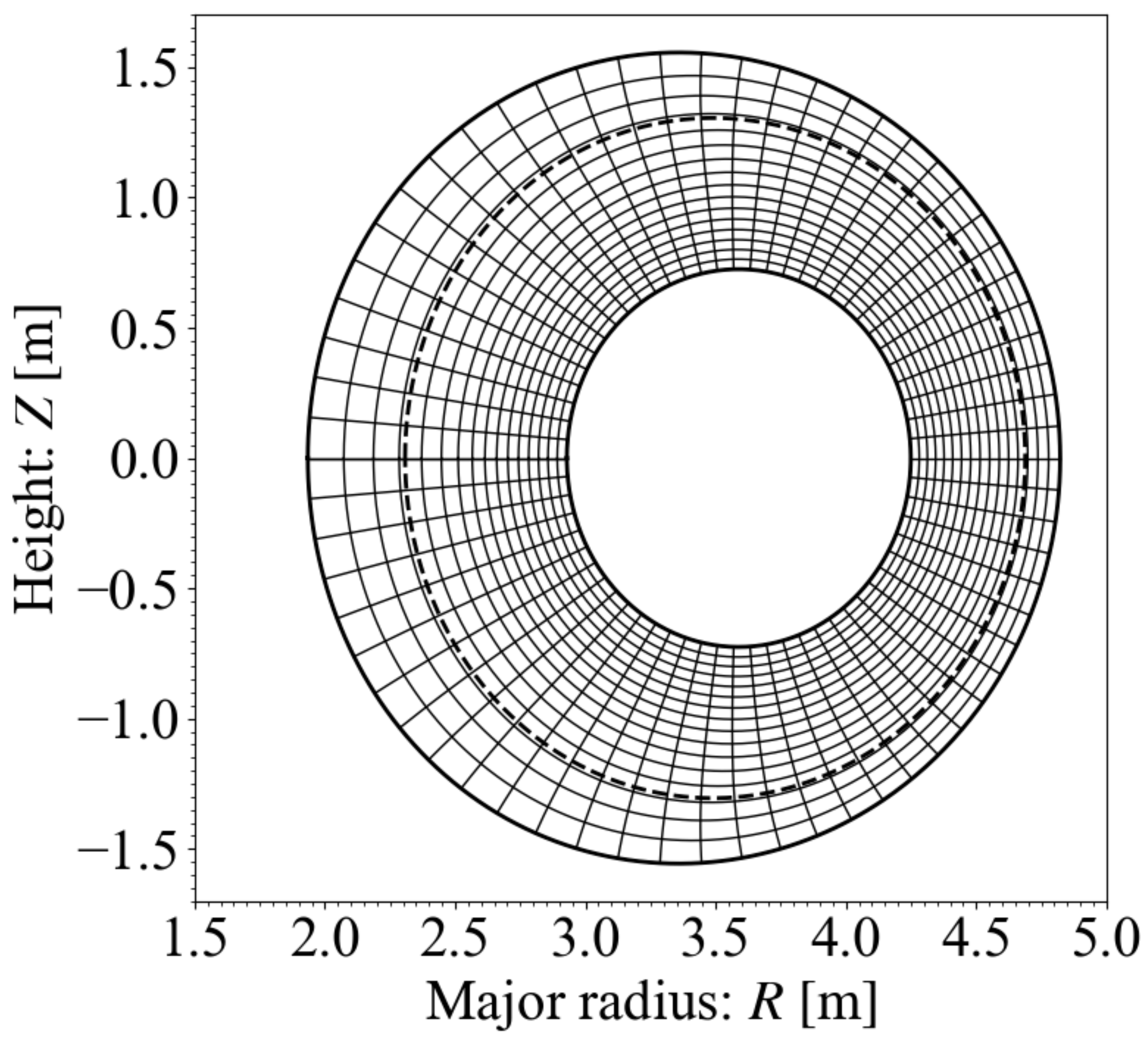

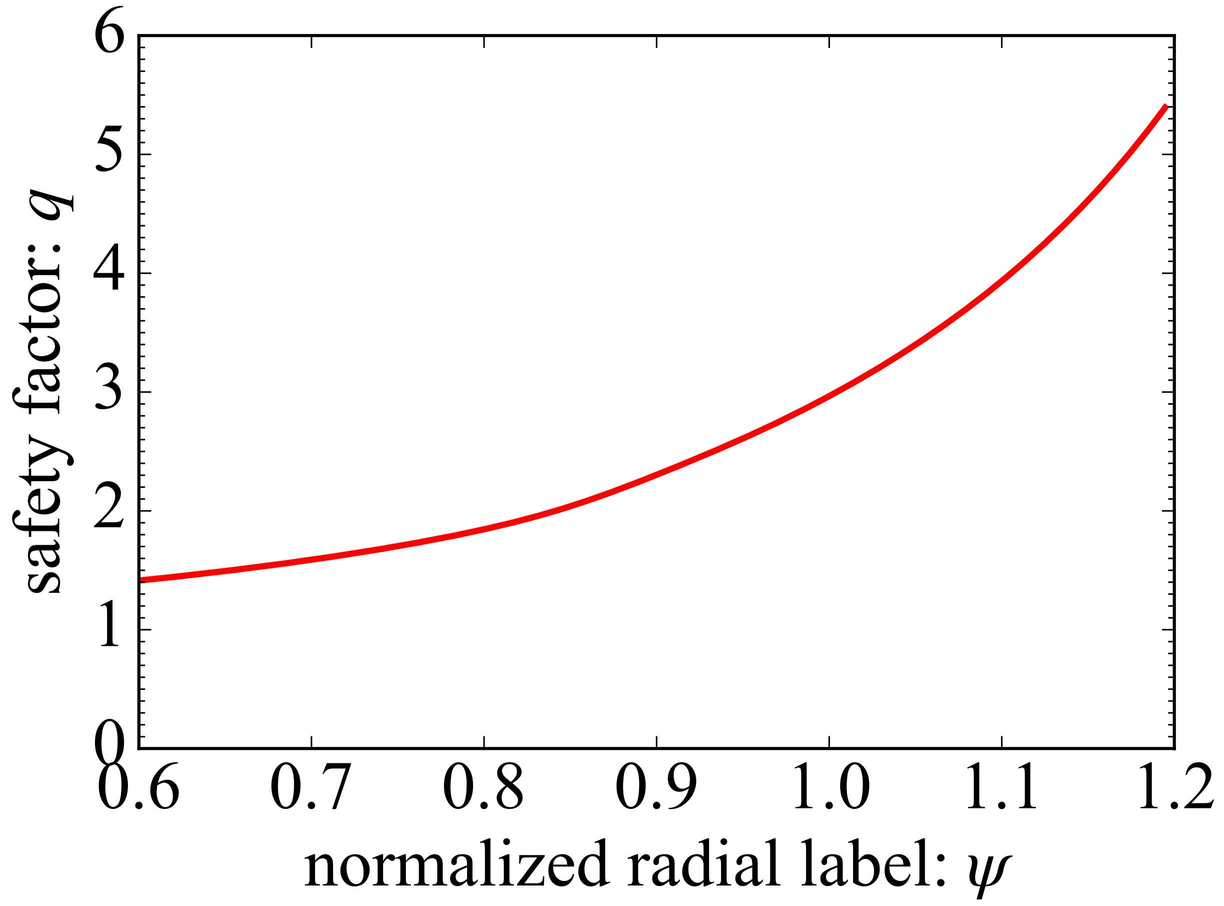

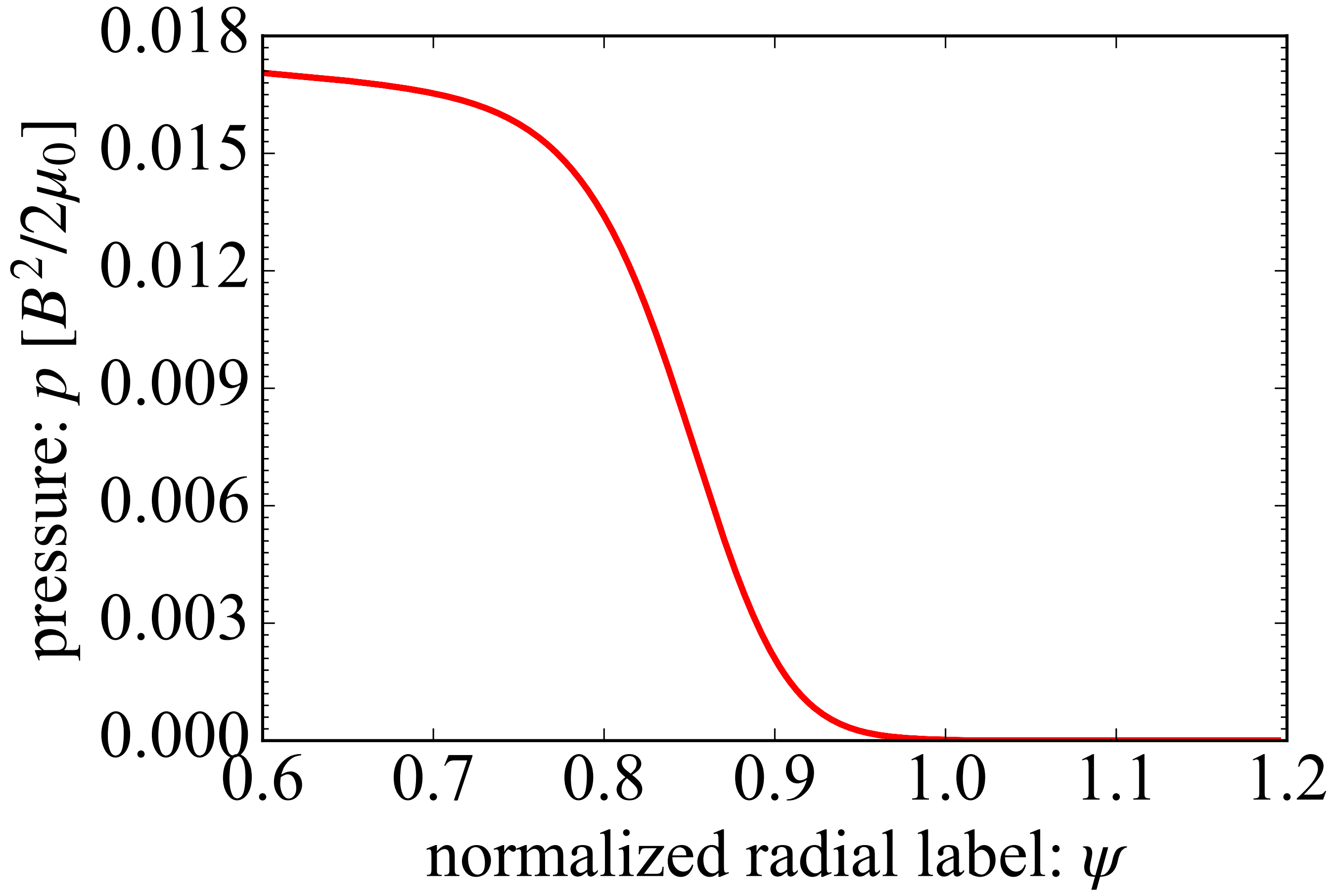

Resolution	Nx	Ny	Nz
1D Poisson	512	64	16
2D Poisson	512	512	16

- $1/n$-th annular wedge domain for $n=5,\ldots,12$
- z-derivatives are evaluated with FFT

[1] Dudson CPC2009, Dudson PPCF2011, Xu NF2011

IBM growth rates by 2D solver show good agreement with those by 1D solver

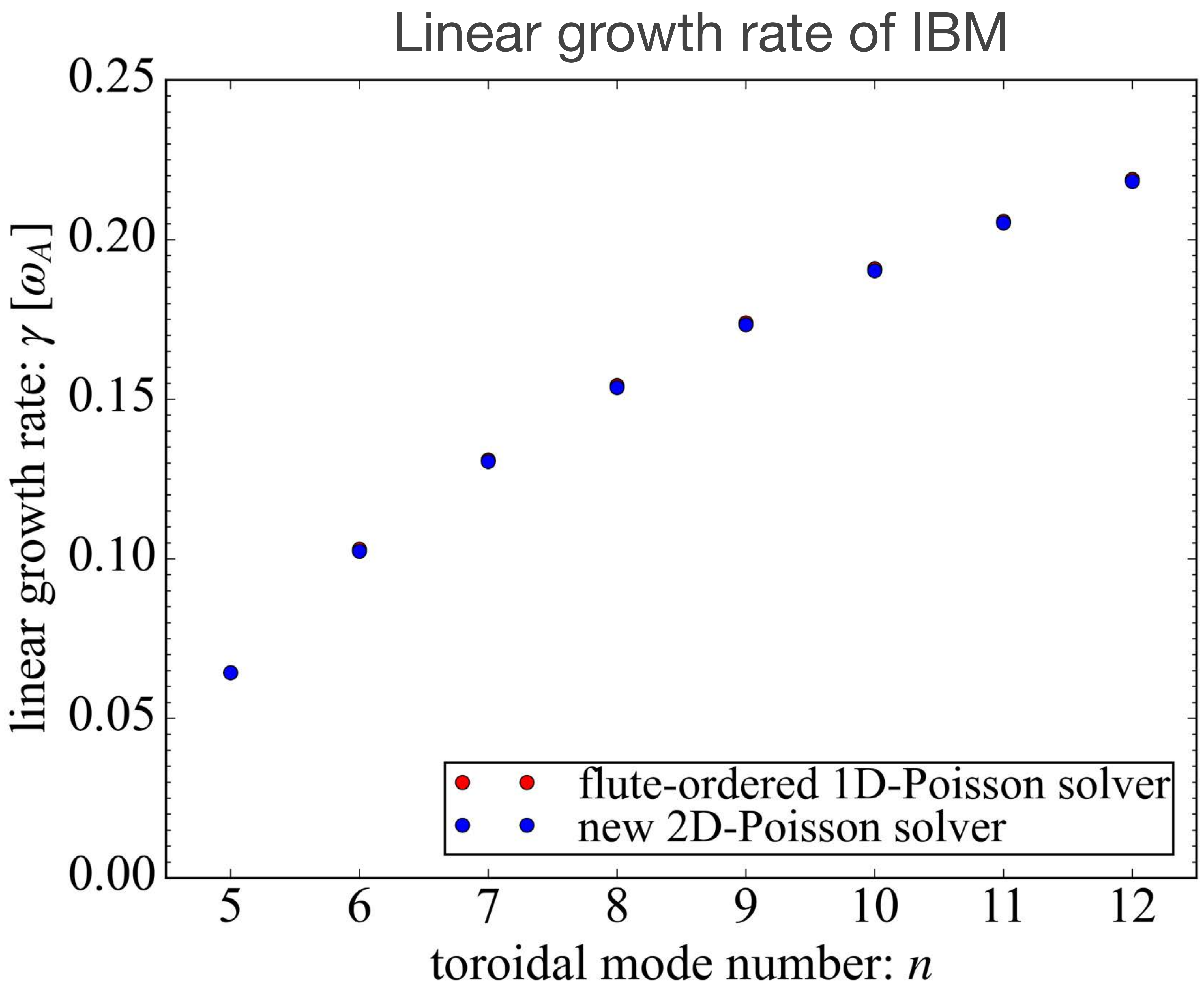

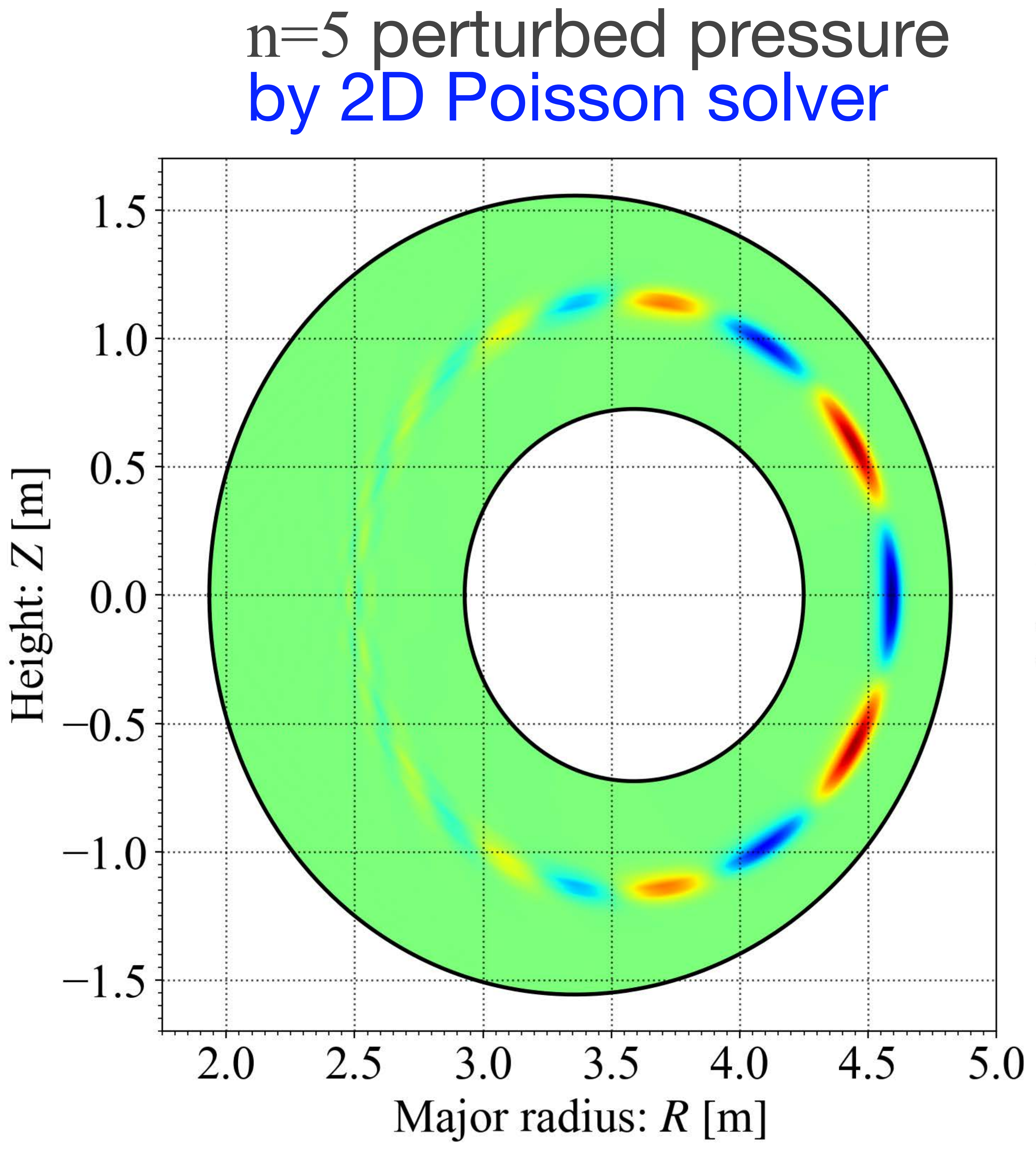

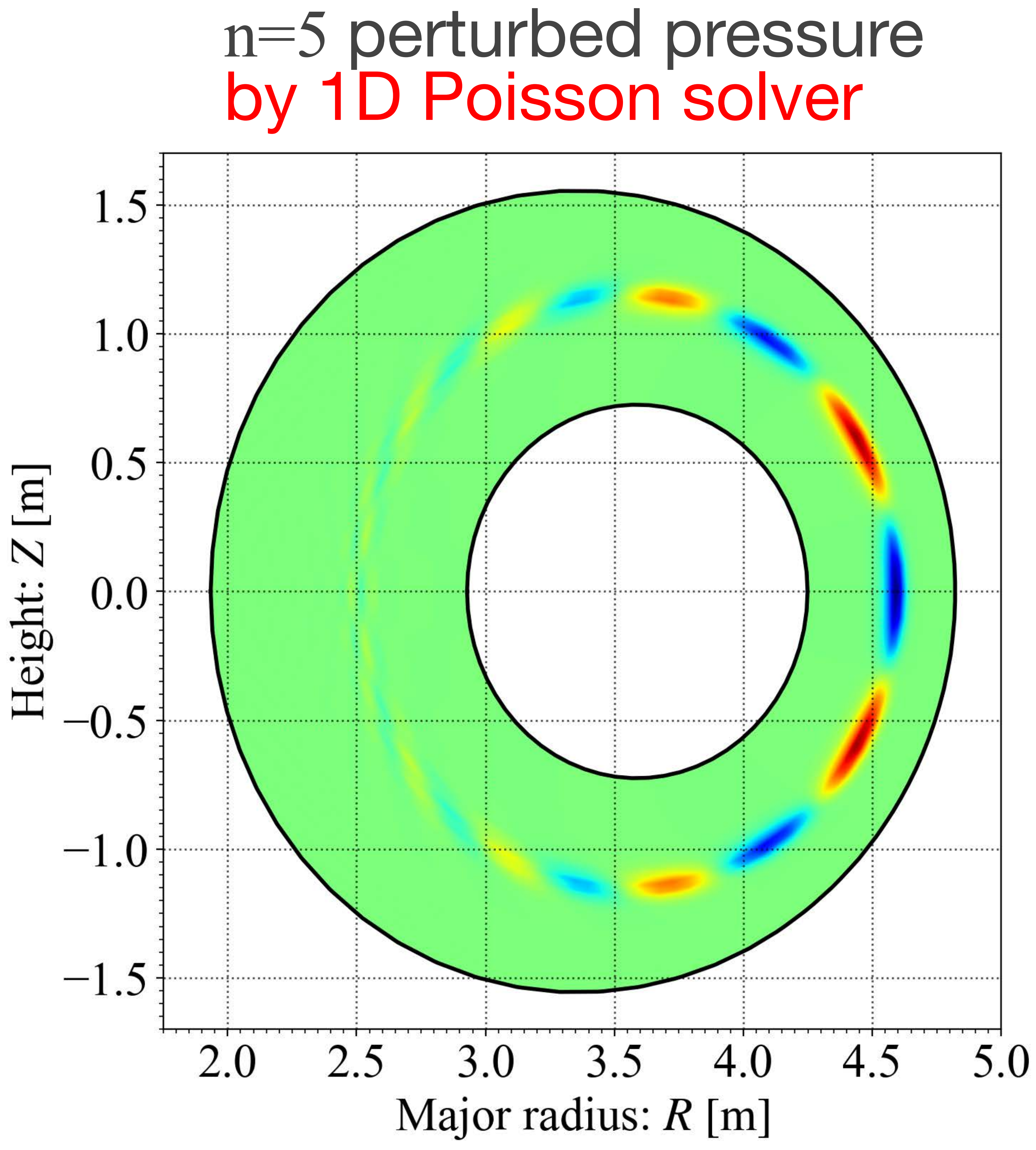

- IBM growth rates show good agreement
- 2D Poisson solver test with current-driven linear instabilities is in preparation

2D Poisson solver test 2: linear resistive ballooning mode in single null geometry

2D Poisson solver is tested in single-null geometry by comparing linear RBM growth rates by 2D Poisson solver and those by1D flute-ordered Poisson solver

Linearized RBM model with dissipation

$$
\begin{aligned}
\frac{\partial \varpi_1}{\partial t} =& B_0 \partial_\parallel \left(\frac{J_\parallel}{B_0} \right) - B_0 \left[A_{1\parallel}, \frac{J_{\parallel 0}}{B_0} \right] + \frac{\boldsymbol{b}_0 \times \boldsymbol{\kappa}_0 \cdot \nabla P_1}{B_0} \\
&+ \mu_\perp \nabla_\perp^2 \varpi_1 + \mu_\parallel \partial_\parallel^2 \varpi_1 \\
\frac{\partial P_1}{\partial t} =& - [\phi_1, P_0] \\
\frac{\partial A_{\parallel 1}}{\partial t} =& - \partial_\parallel \phi_1 + \eta J_{\parallel 1} \\
\varpi =& \nabla \cdot \left(\frac{1}{B_0^2} \nabla_\perp \phi \right), \quad J_{\parallel 1} = \nabla_\perp^2 A_{\parallel 1}
\end{aligned}
$$

$$\eta = 10^{-6}, \quad \mu_\perp = 10^{-7}, \quad \mu_\parallel = 10^{-1}$$

- constant ion density $n_{i0} = 10^{19}$ [m^{-3}]
- Dissipations in vorticity equation are required for numerical stability in both 2D and 1D Poison solver.

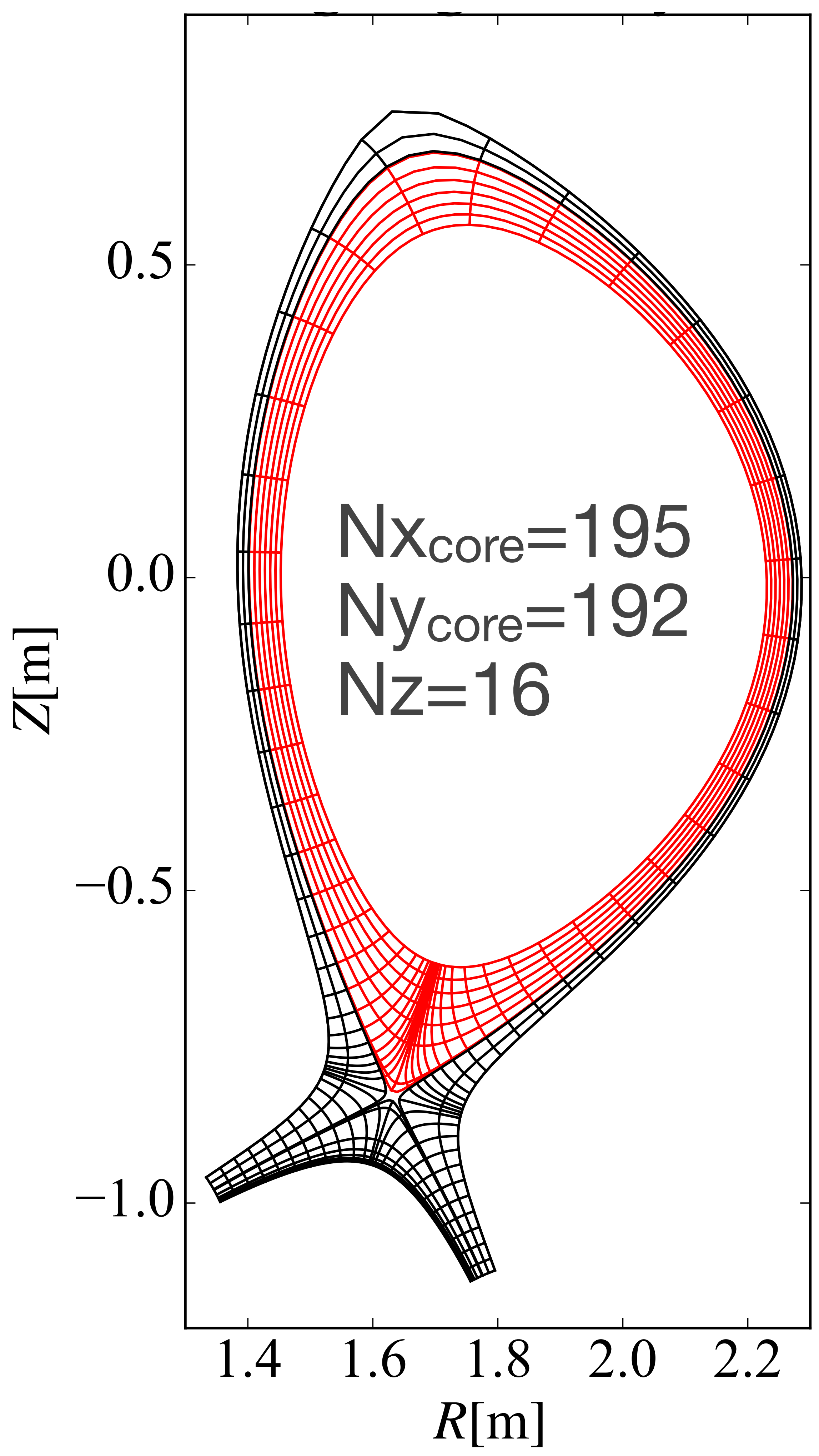

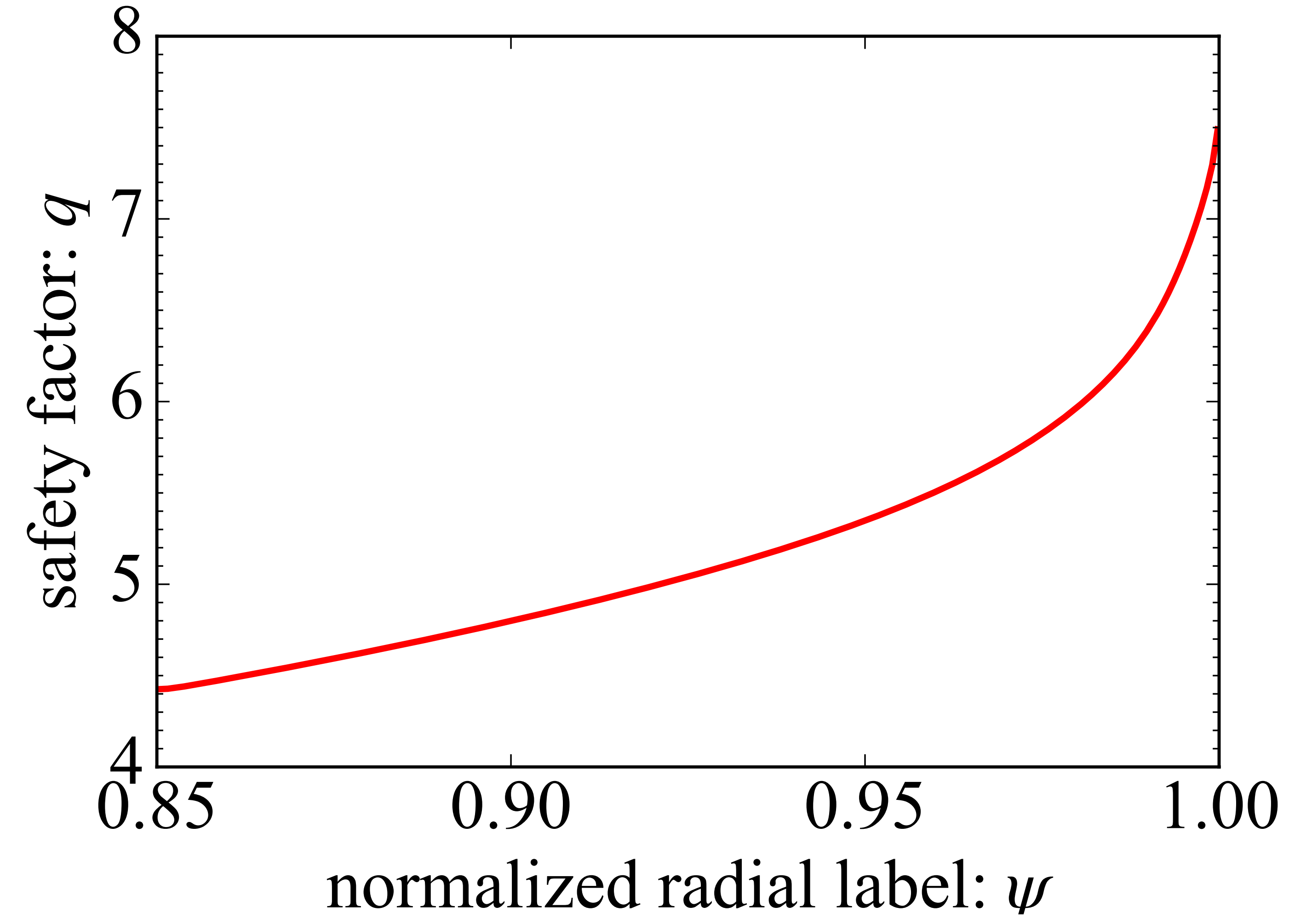

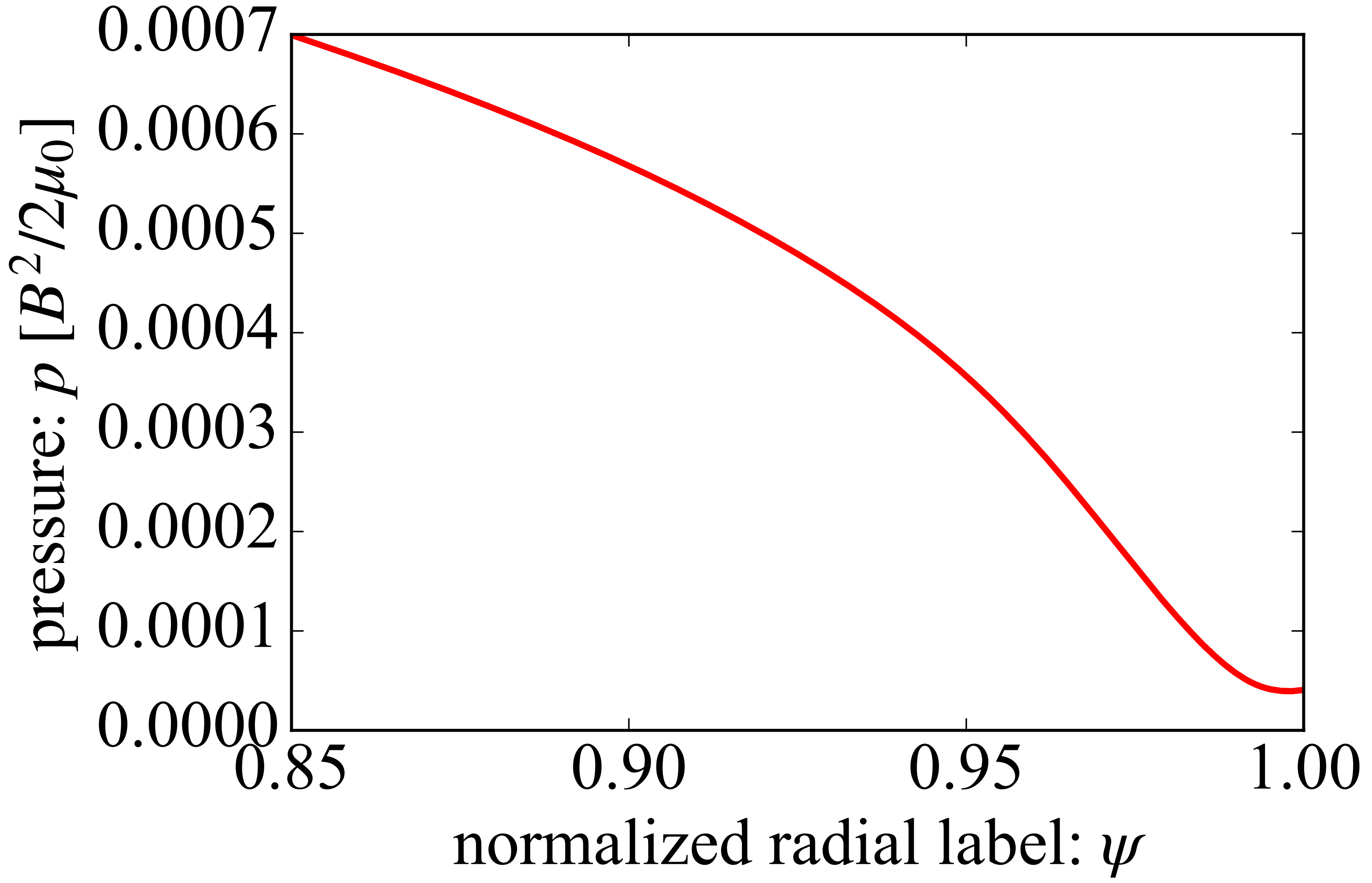

- $1/n$-th annular wedge domain for n=3,4
- z-derivatives are evaluated with FFT

2D Poisson solver captures RBM instability but growth rates are different

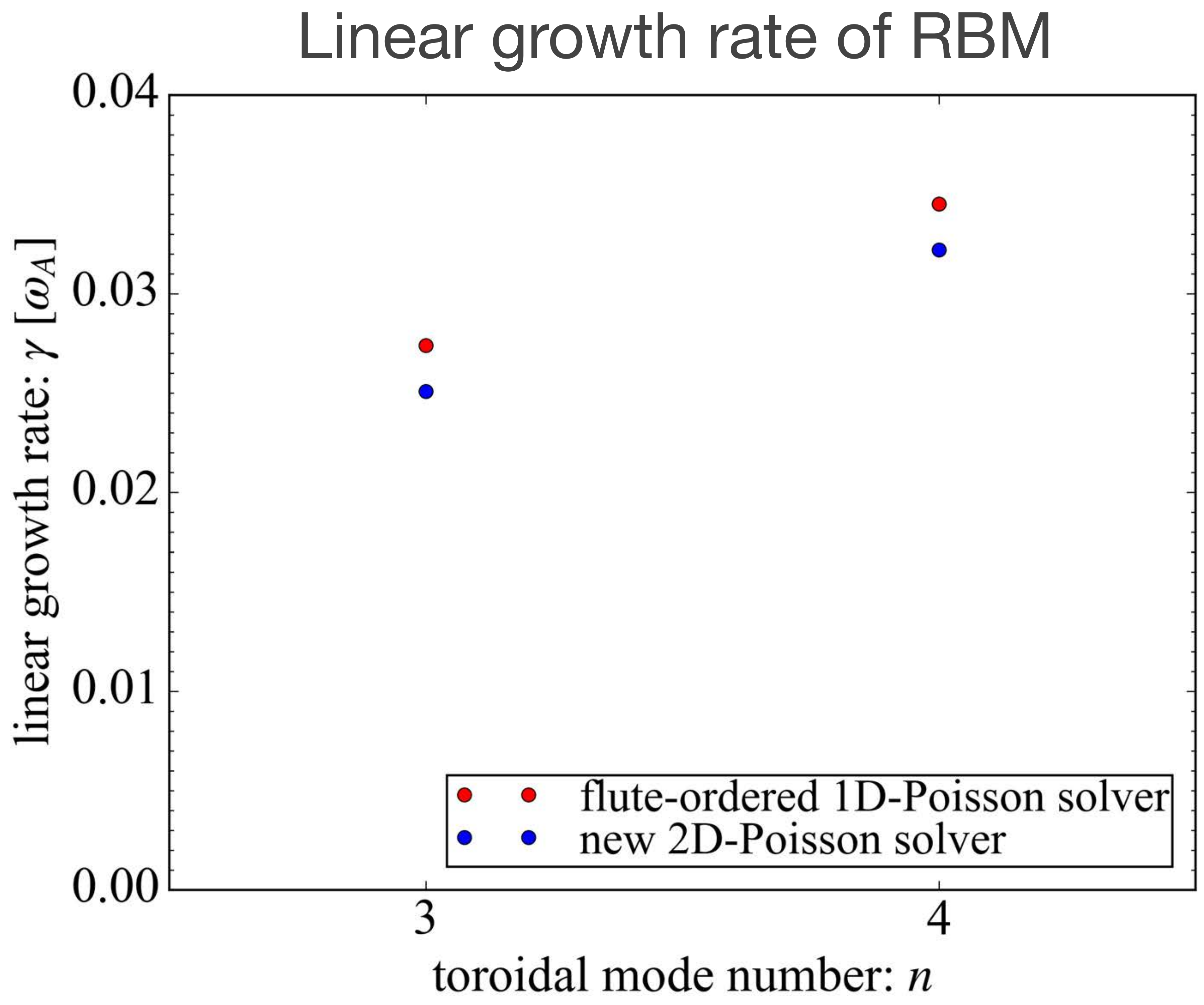

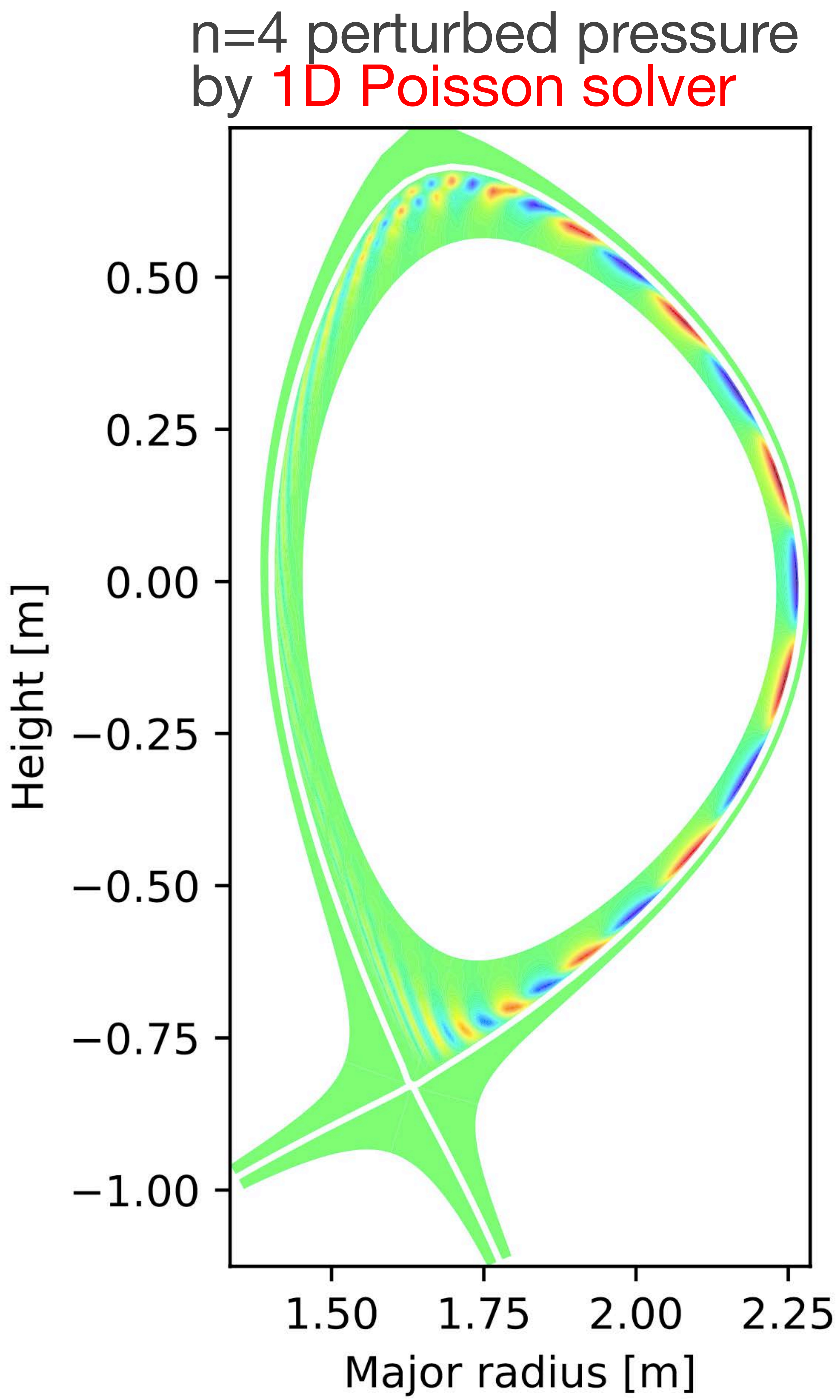

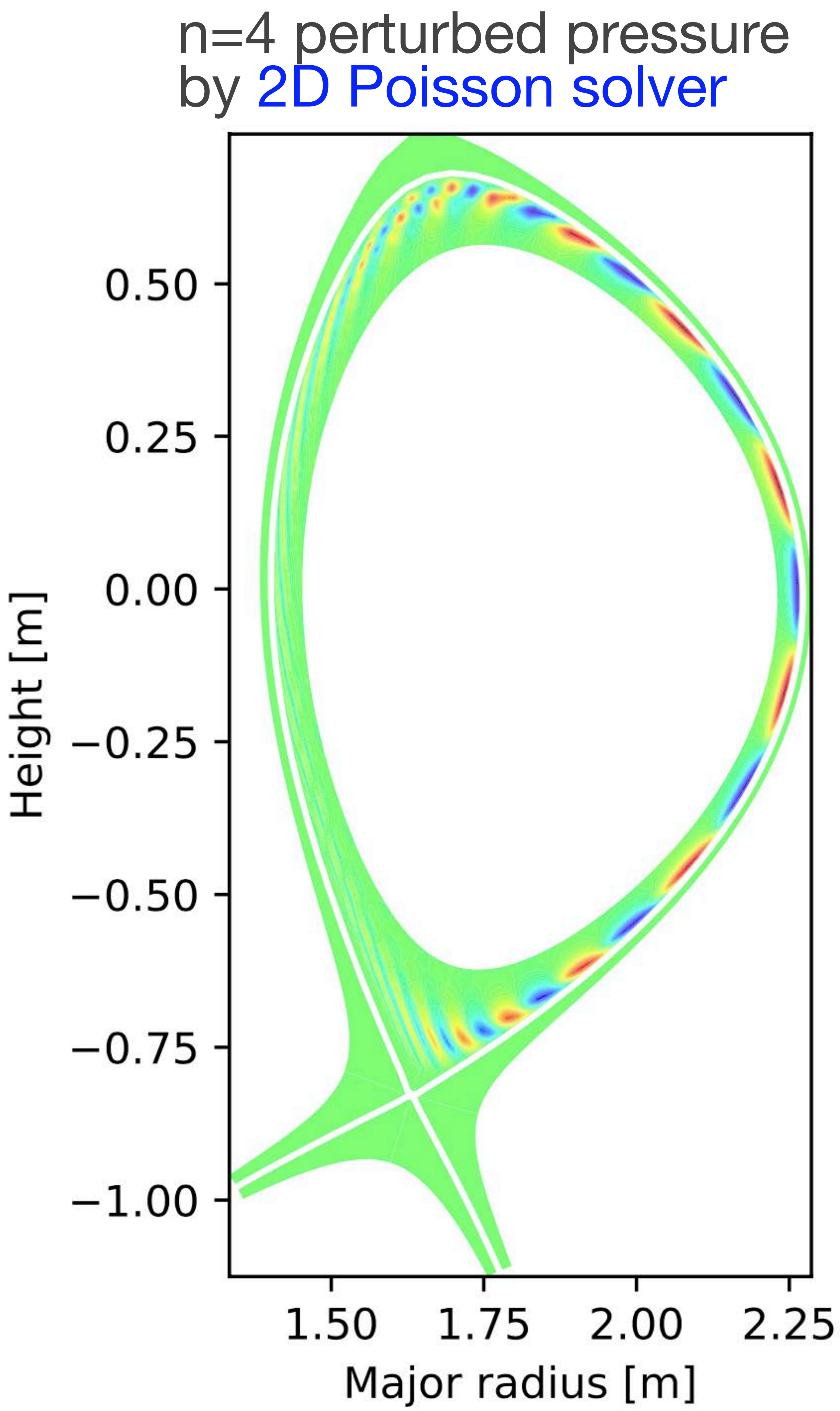

RBM eigen-functions are clearly obtained by both Poisson solvers but their growth rates are different by 6~8%

➡Further tests (mesh convergence etc…) are required to clarify impact of flute-ordering in complex geometries

Outline

- Introduction: BOUT++ code and objectives of TOKEDGE project
- Numerical Issue on Poisson solvers in BOUT++ and a new 2D Poisson solver for low-n modes
- Verification test of 2D Poisson solver by linear problems (pressure-driven modes)
- Preliminary pedestal collapse simulation in annular full tours domain in shifted circular geometry
- Summary and future work (research plan in FY2021)

Pedestal collapse by resistive ballooning mode in a shifted circular geometry

four-field RMHD model: RBM+drift wave [Seto CPP2020]

$$
\begin{aligned}
\frac{\partial}{\partial t}\varpi_1 &= -\left[F_1, \varpi\right] - \left[F_0, \varpi_1\right] + \mathcal{G}\left(p_1, F\right) + \mathcal{G}\left(p_0, F_1\right) - B_0\partial_\parallel\left(\frac{J_{\parallel 1}}{B_0}\right) + B_0\left[A_{\parallel 1}, \frac{J_\parallel}{B_0}\right] + \mathcal{K}(p_1) + \mu_\parallel \partial_\parallel^2 \varpi_1 + \mu_\perp \nabla_\perp^2 \varpi_1, \\
\frac{\partial}{\partial t}p_1 &= -\left[\phi_1, p\right] - \left[\phi_0, p_1\right] - 2\beta_*\left(\mathcal{K}(p_1) - B_0\partial_\parallel\left(\frac{v_{\parallel 1} + d_i J_{\parallel 1}}{2B_0}\right) + B_0\left[A_{\parallel 1}, \frac{v_{\parallel 1} + d_i J_{\parallel 1}}{2B_0}\right]\right) + \chi_\parallel \partial_\parallel^2 p_1 + \chi_\perp \nabla_\perp^2 p_1, \\
\frac{\partial}{\partial t}A_{\parallel 1} &= -\left[\phi, A_{\parallel 1}\right] - \partial_\parallel \phi_1 + \delta_e\left(\partial_\parallel p_1 - \left[A_{\parallel 1}, p\right]\right) + \eta J_{\parallel 1} - \lambda \nabla_\perp^2 J_{\parallel 1}, \\
\frac{\partial}{\partial t}v_{\parallel 1} &= -\left[\phi, v_{\parallel 1}\right] - \frac{1}{2}\left(\partial_\parallel p_1 - \left[A_{\parallel 1}, p\right]\right) + \nu_\perp \nabla_\perp^2 v_{\parallel 1},
\end{aligned}
$$

$$
\varpi = \nabla_\perp^{*2} F, \quad J_1 = \nabla_\perp^2 A_\parallel, \quad F = \phi + \delta_i p, \quad \phi = \phi_0 + \phi_1, \quad p = p_0 + p_1, \quad \boldsymbol{B} = \boldsymbol{B}_0 + \nabla A_{\parallel 1} \times \boldsymbol{b}_0, \quad J_\parallel = J_{\parallel 0} + J_{\parallel 1},
$$

$$
n_{i0} = 10^{19}\ [m^{-3}], \quad \eta = 10^{-8}, \quad \lambda = 10^{-12}, \quad \mu_\perp = \chi_\perp = \nu_\perp = 10^{-7}, \quad \mu_\parallel = \chi_\parallel = 10^{-1}
$$

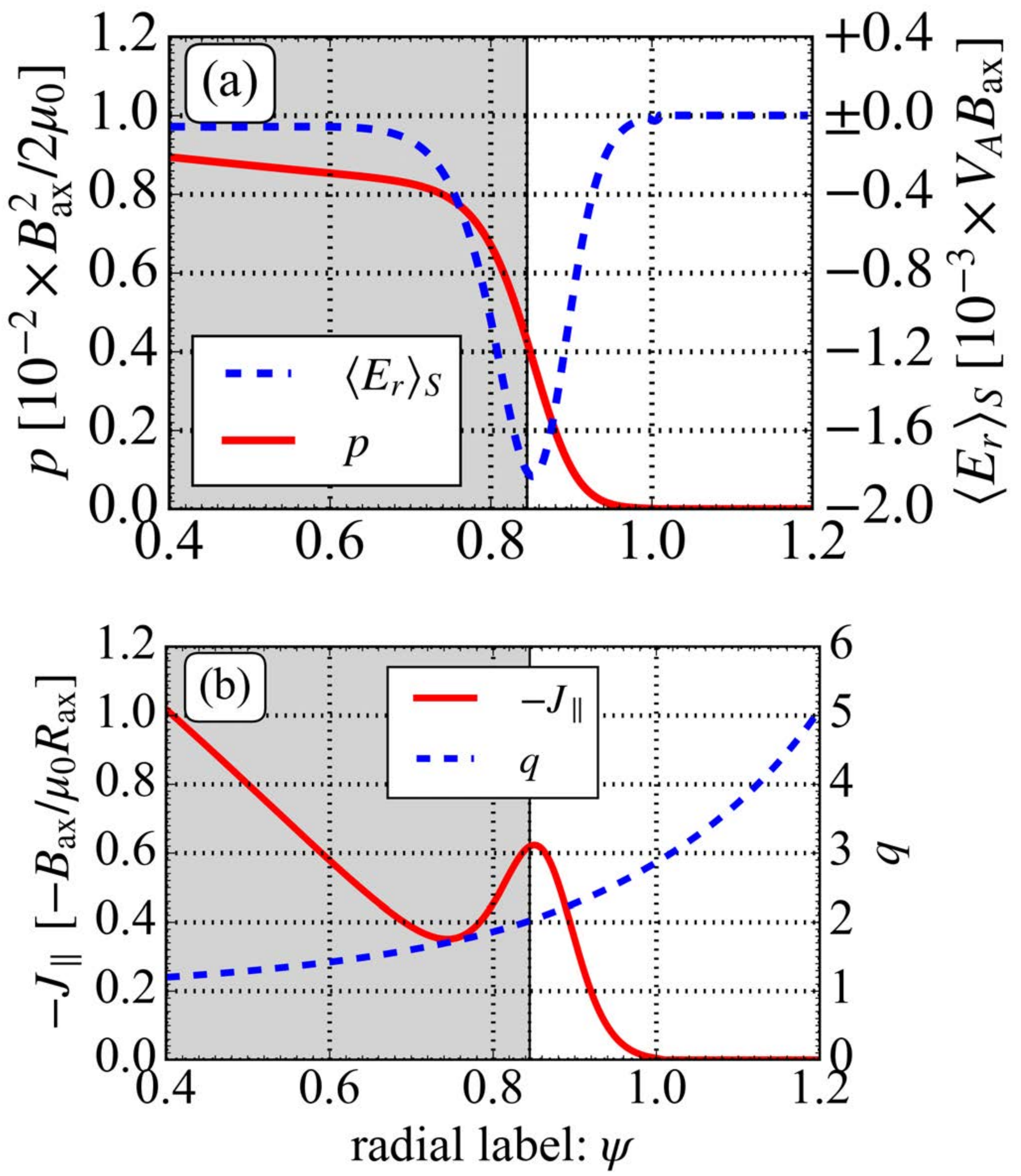

IBM marginally stable shifted circular equilibrium

- Resolution: Nx=512, Ny=128, Nz=256 (n=0,1,…,80) for full annular tours
  - n=0,1,2,3,4 modes are solved with 2D Poisson solver without flute-ordering
  - n=5,6,…,80 modes are solved with 1D Poisson solver with flute-ordering
- just for test run and radial and toroidal resolution may not be not enough for production run
  - cf.) Nx=1536, Ny=64, Nz=129 for 1/5th annular tours (n=0,5,…155,160) in Seto CPP2020

Pedestal collapse is trigged by n~30 resistive ballooning modes

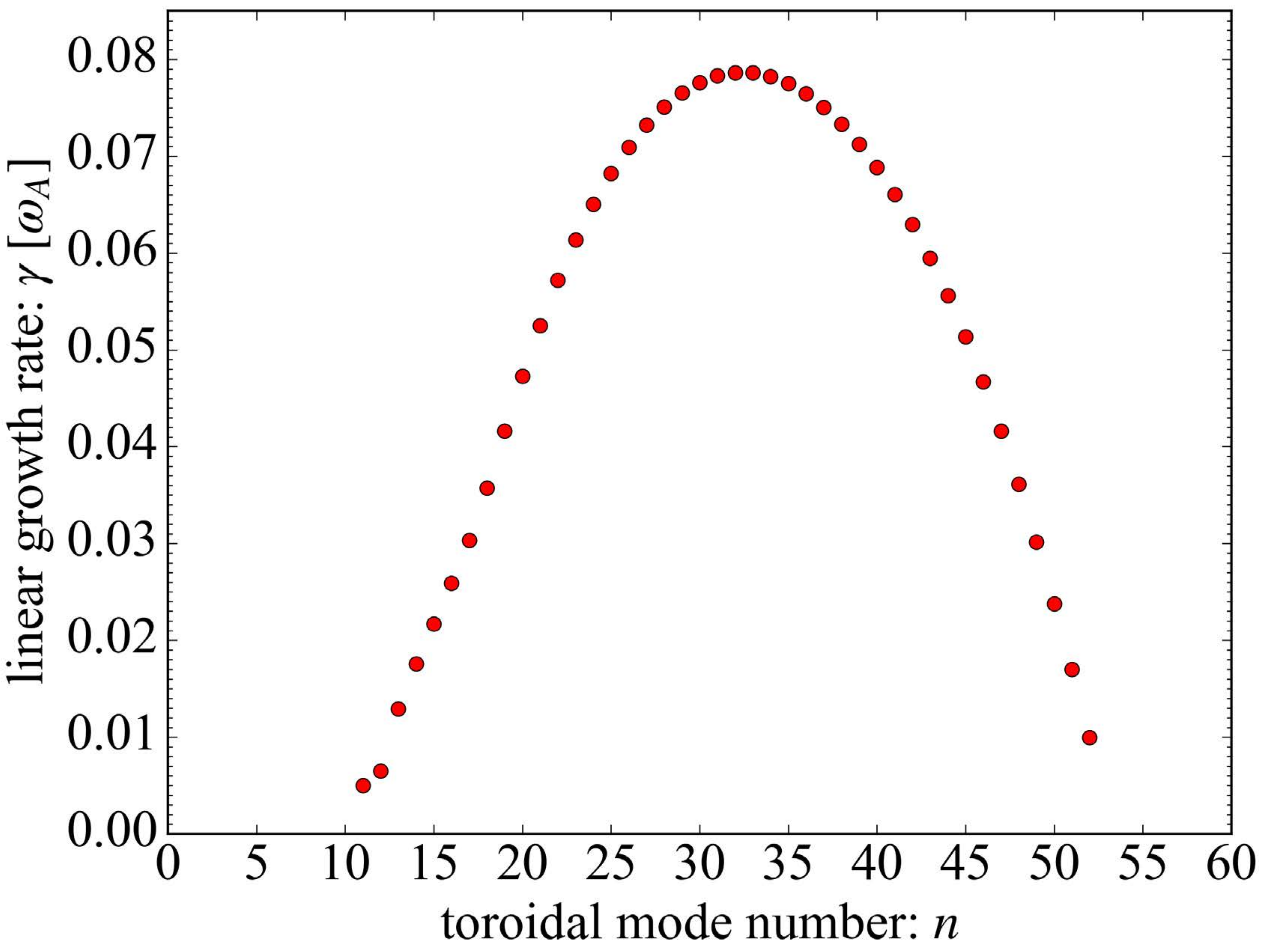

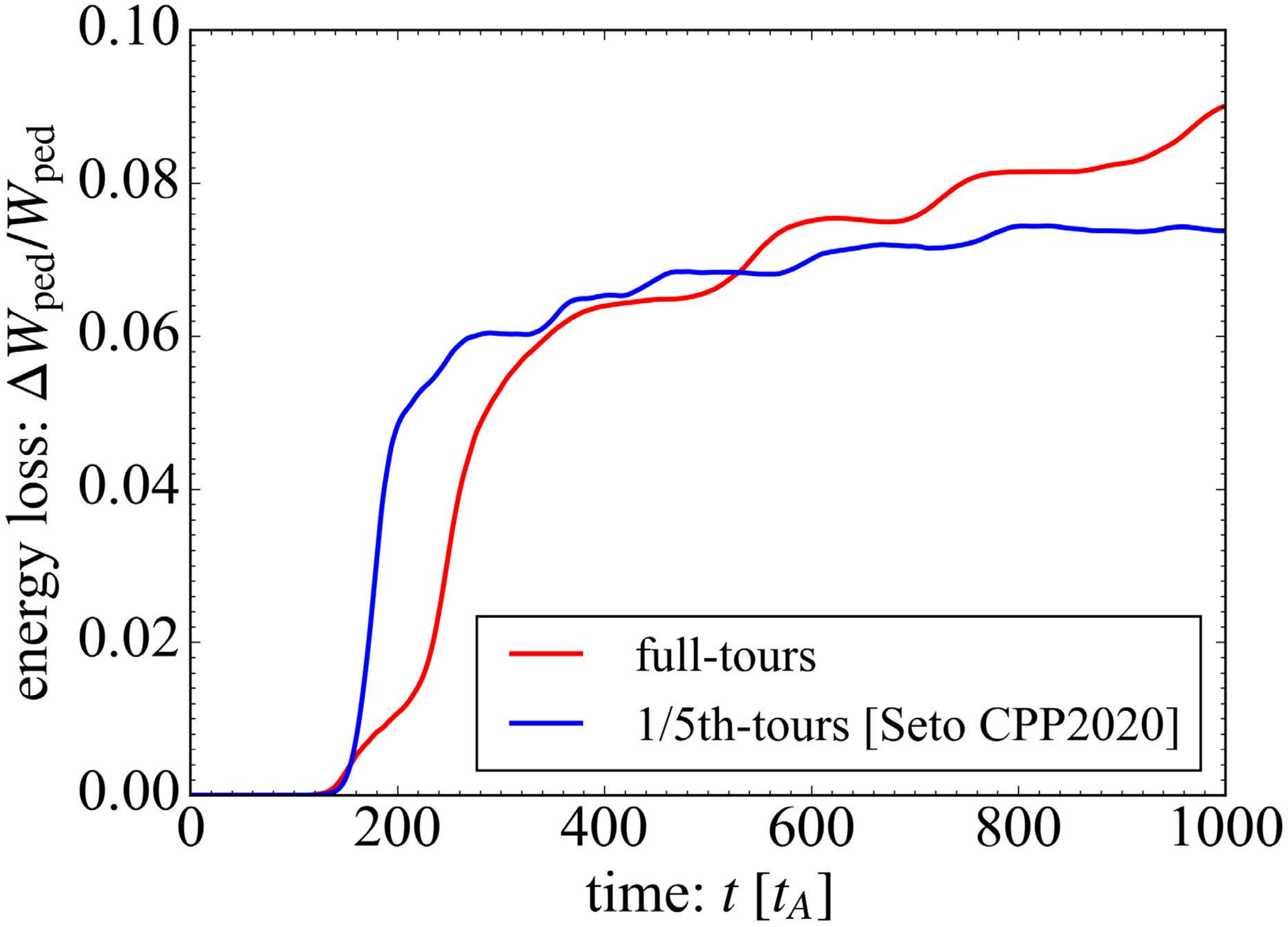

Computational cost for full tours simulation: 2048core x 2day in JFRS1

Energy loss dynamics during pedestal collapse changes qualitatively

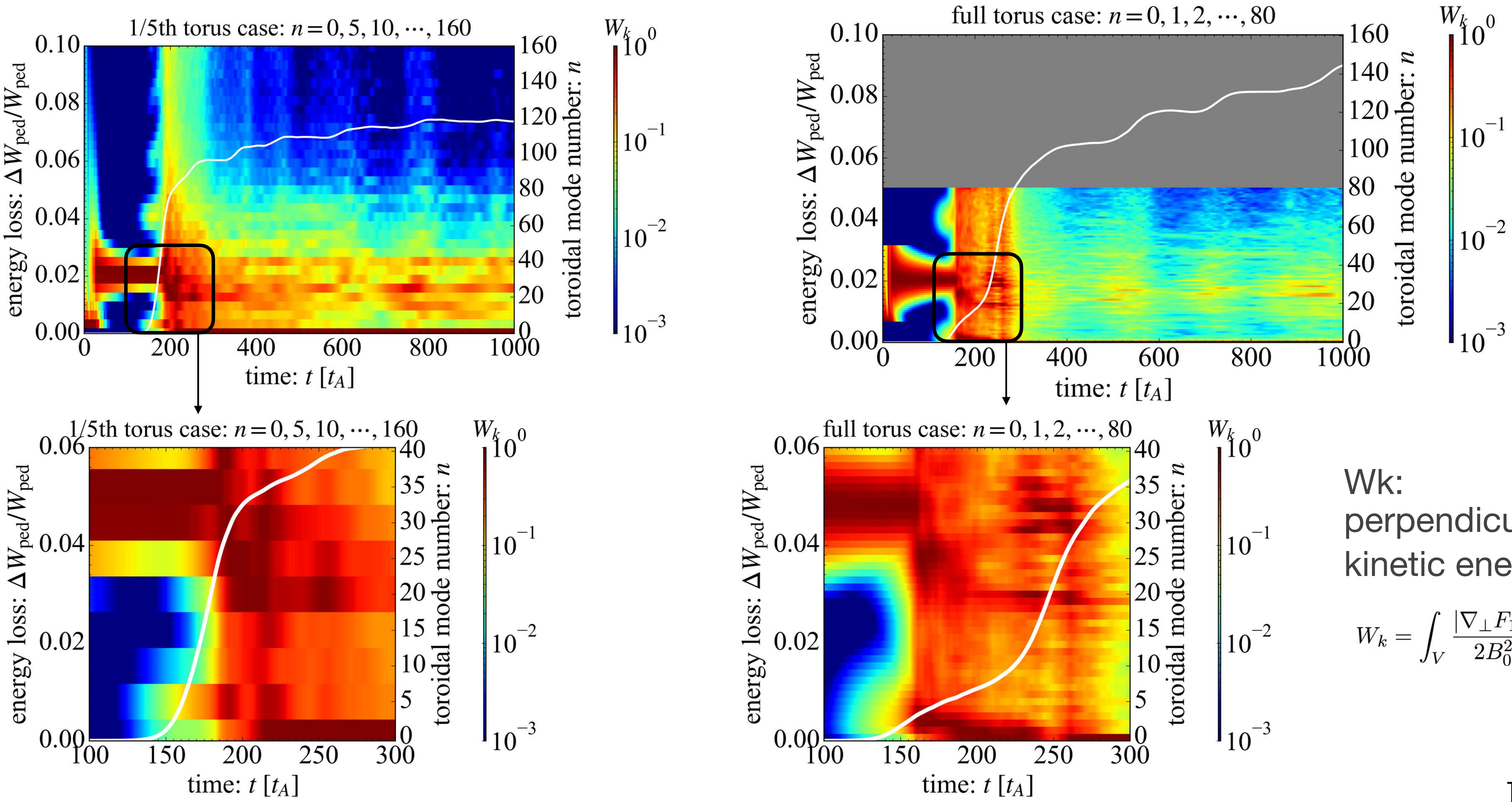

Wk: perpendicular kinetic energy

$$W_k = \int_V \frac{|\nabla_\perp F_1|^2}{2B_0^2} dV$$

Time evolution of perpendicular kinetic energy from n=0 to n=80

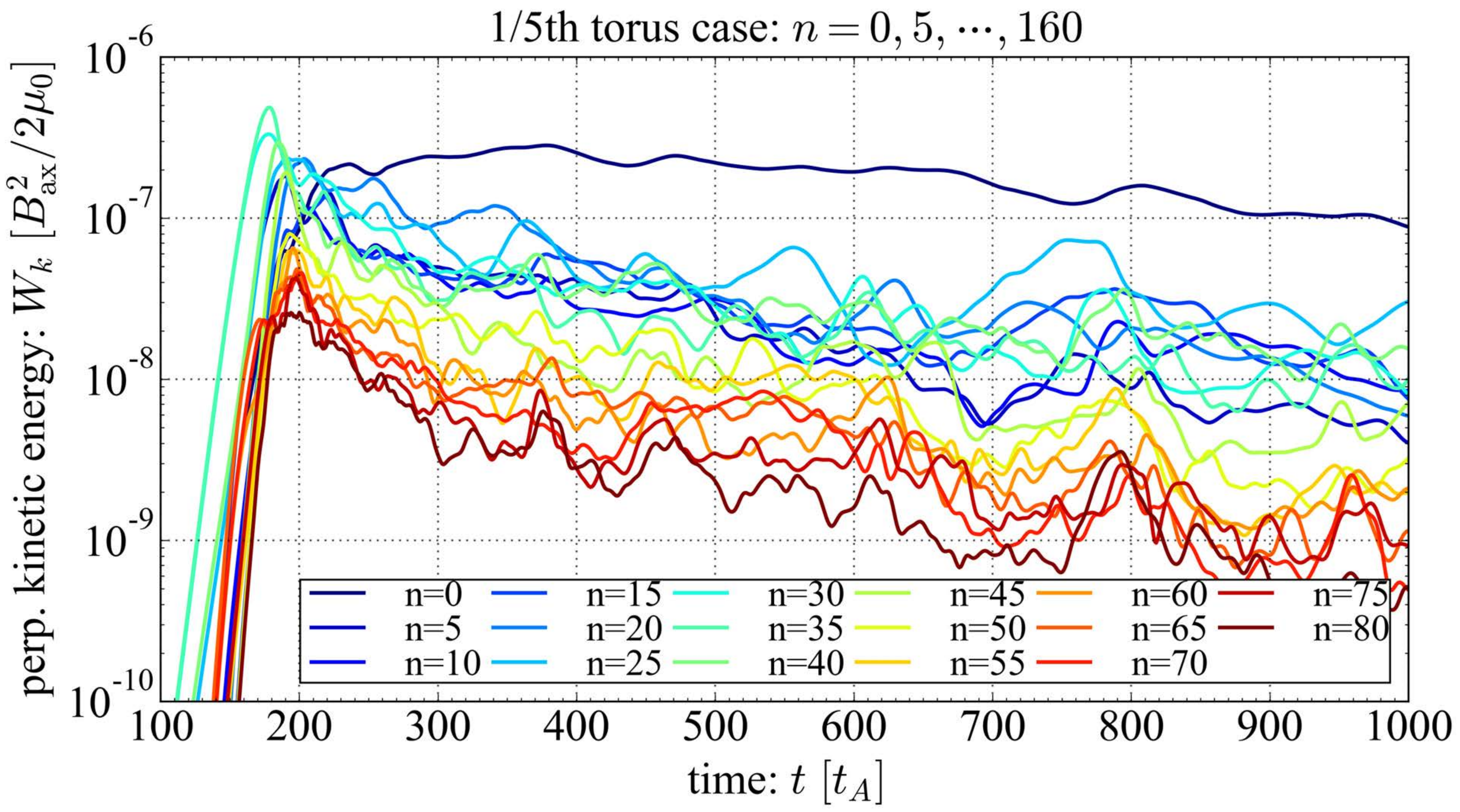

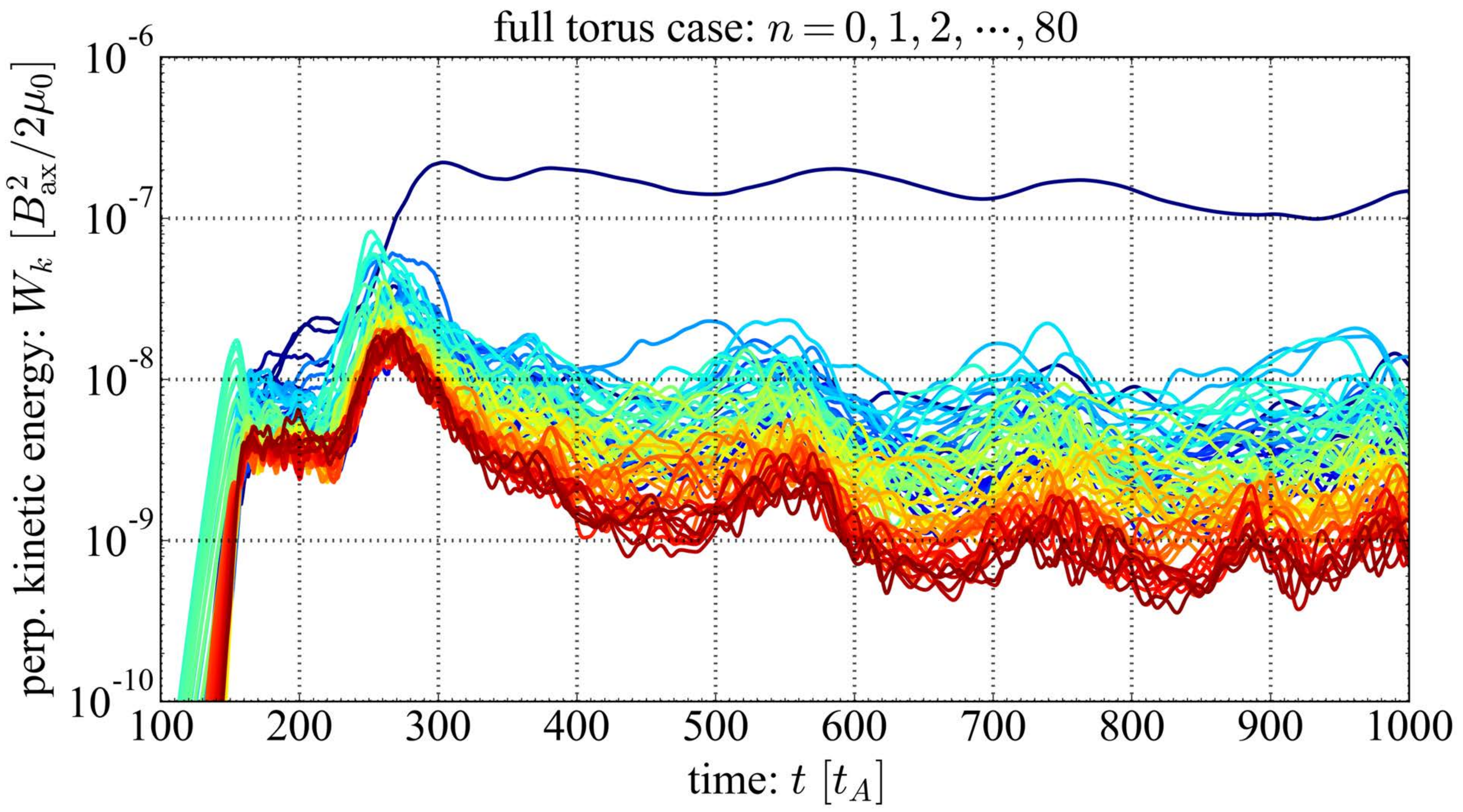

- Amplitude of kinetic energy of most unstable mode decreases by one order in full torus case

  ➡increase of unstable toroidal modes driving pedestal collapse in simulated system

- Amplitude of zonal flow (n=0 energy) after pedestal collapse are similar order O(10^{-7})

- Pedestal collapse has two phases in full torus case

perpendicular kinetic energy spectrums just before 1st crash show similar trend

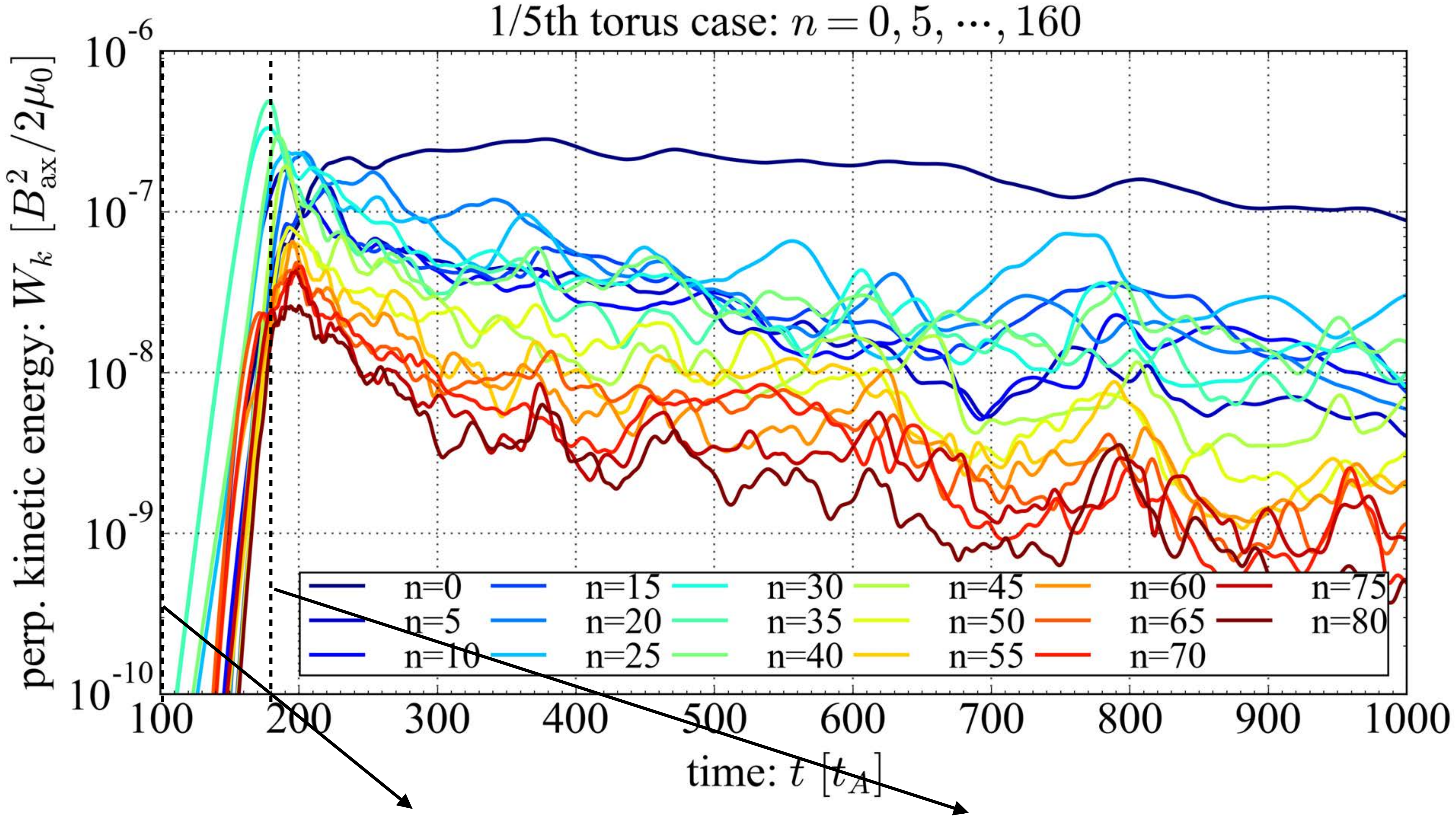

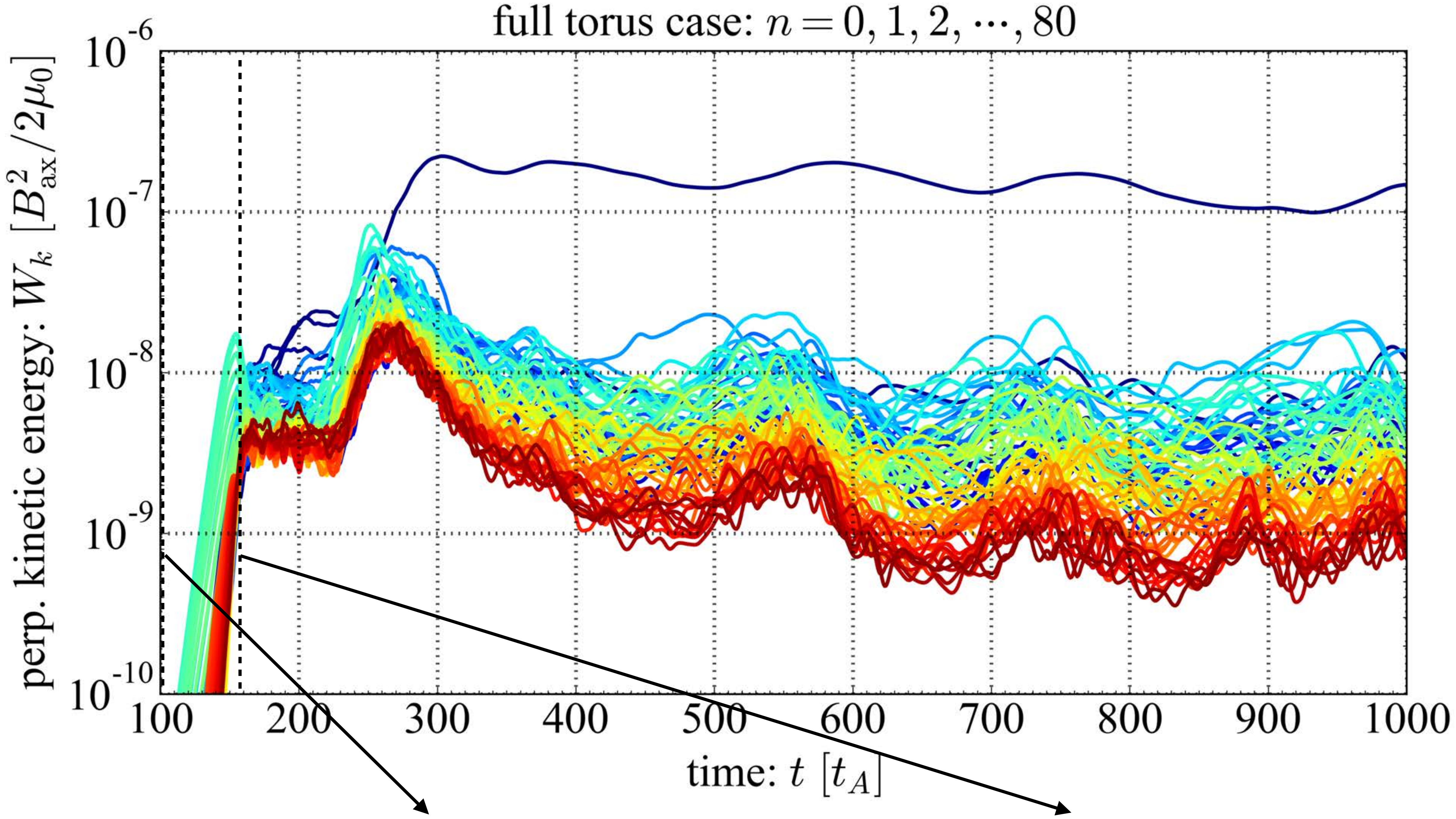

Linear phase: t=100tA

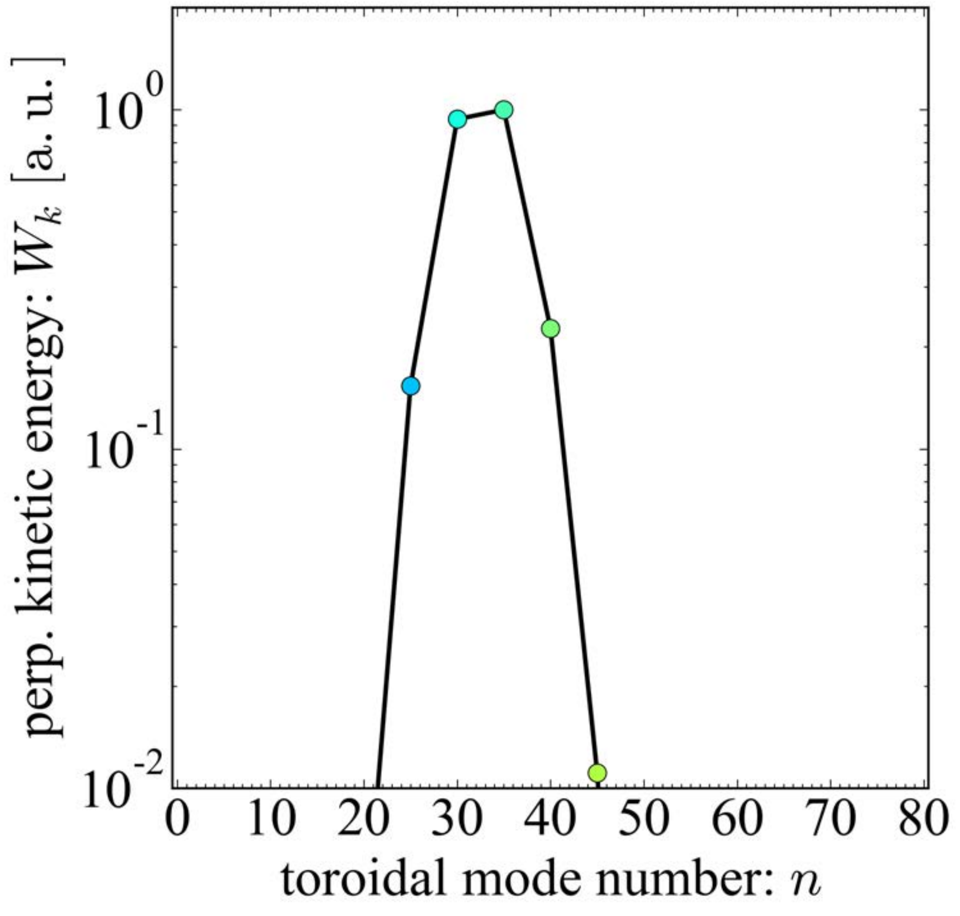

Just before collapse: t=180tA

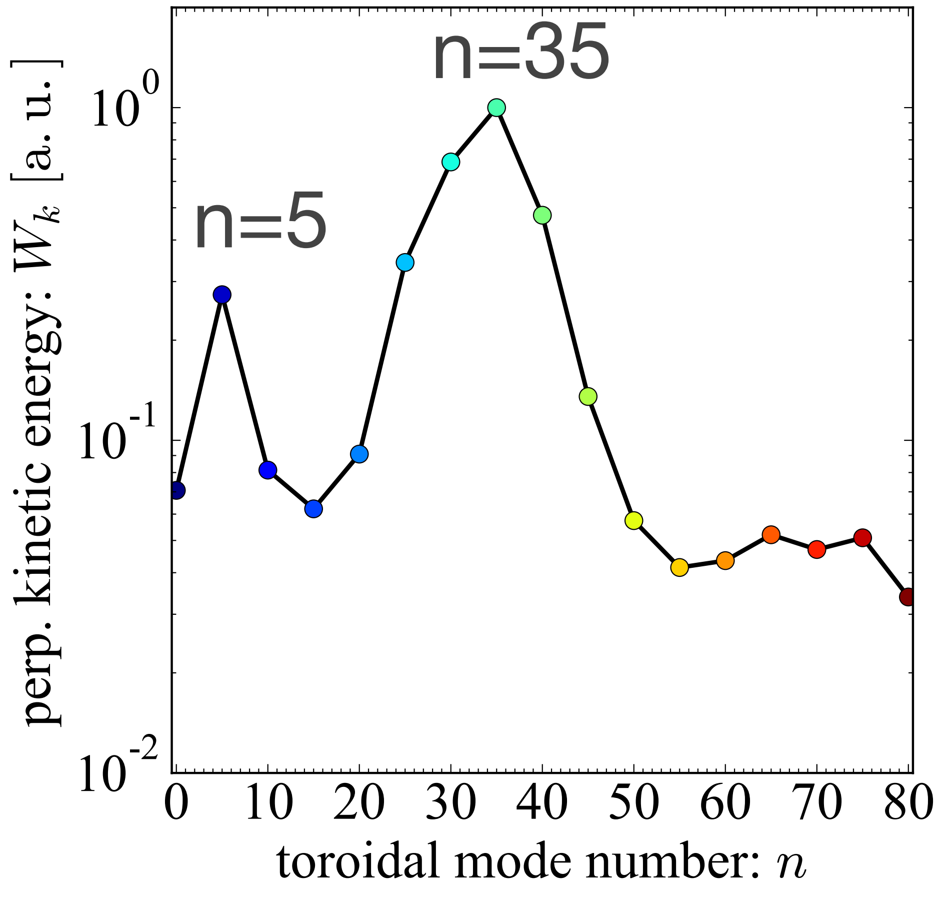

Linear phase: t=100tA

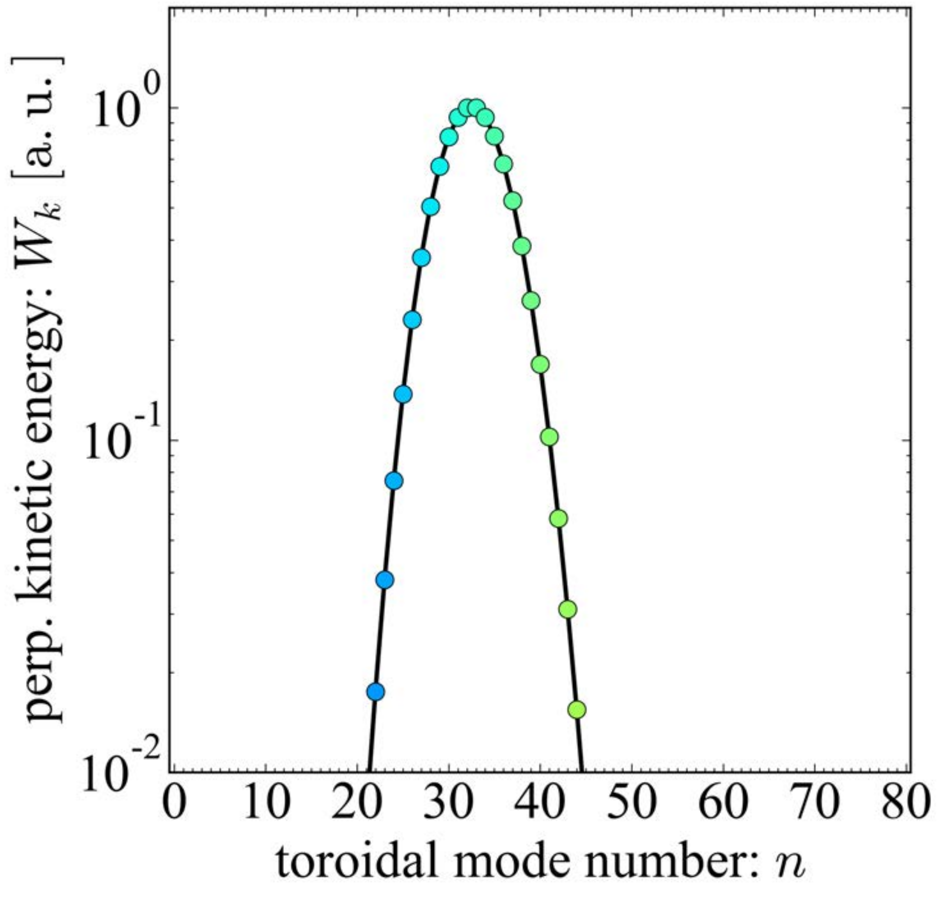

Just before 1st collapse: t=155tA

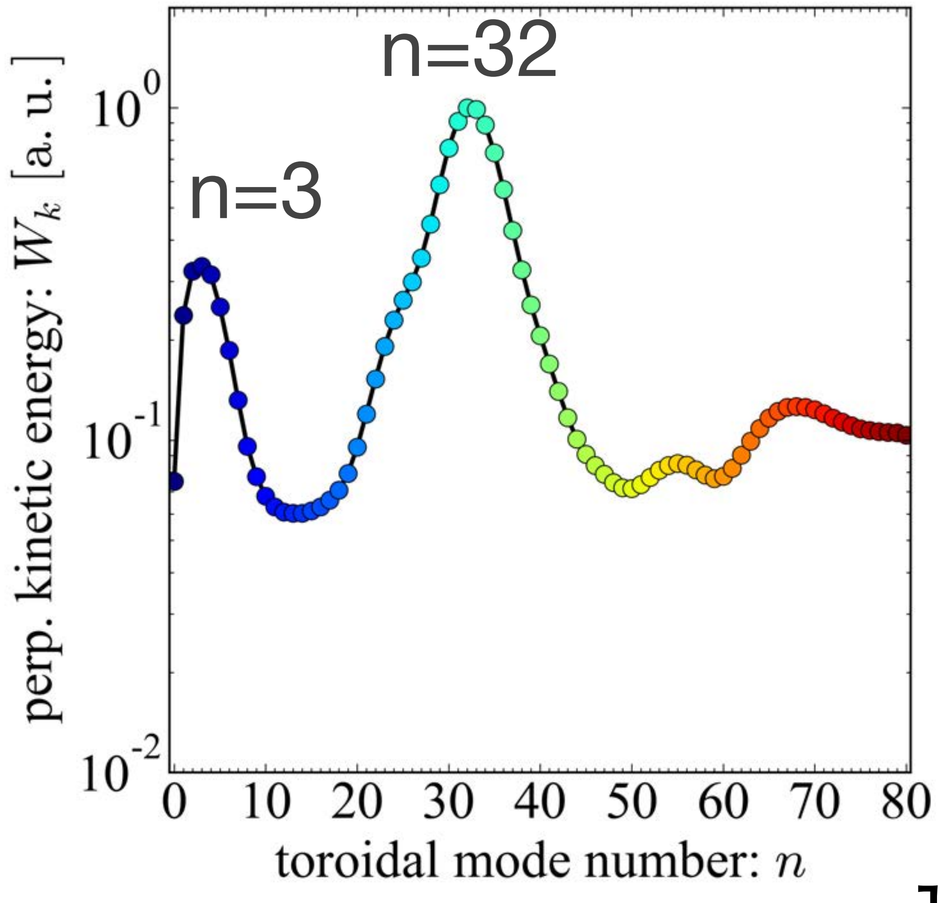

Low-n modes may play a role between two crashes in full torus case

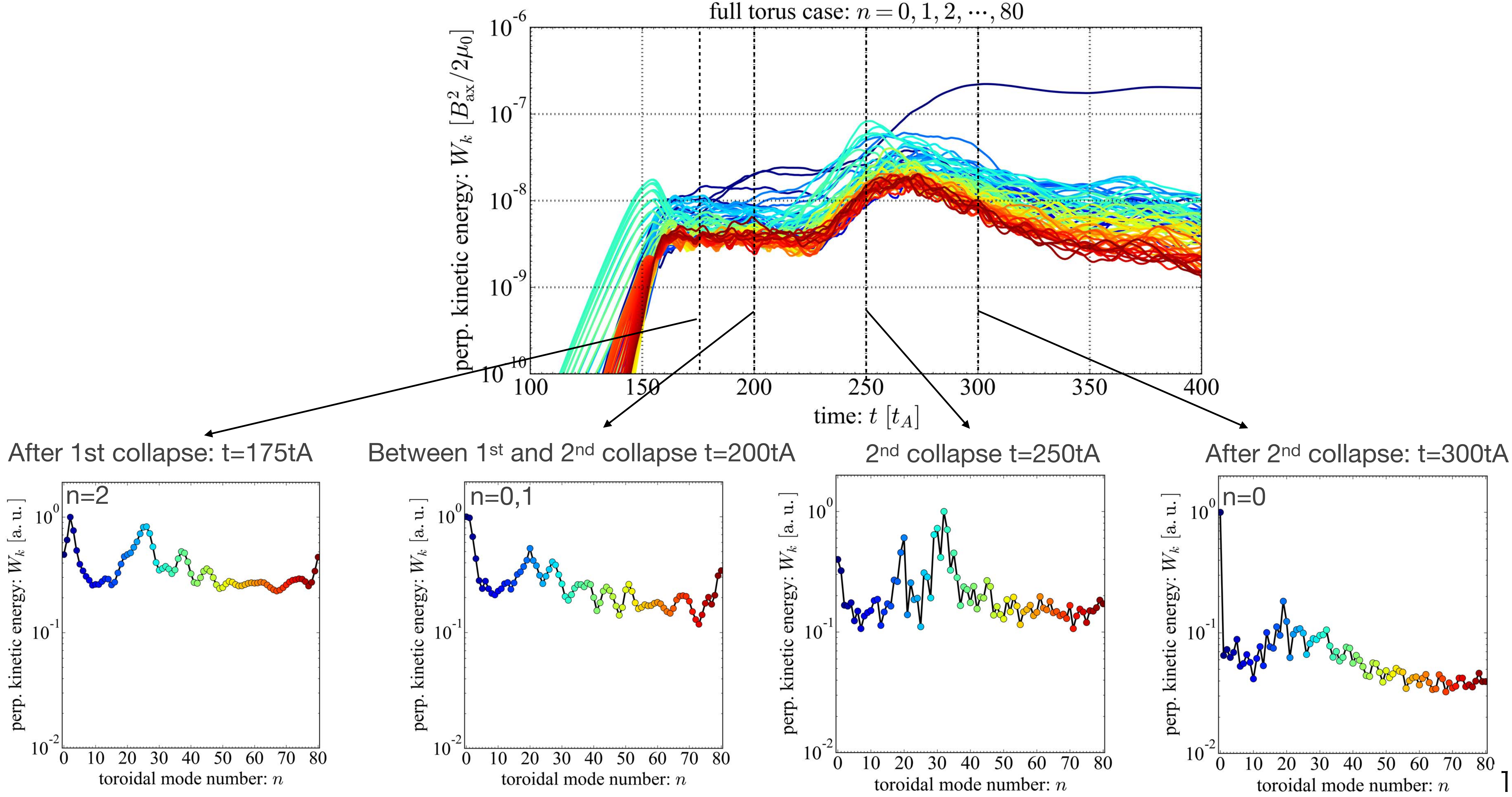

perpendicular kinetic energy spectrums after crashes show similar trend

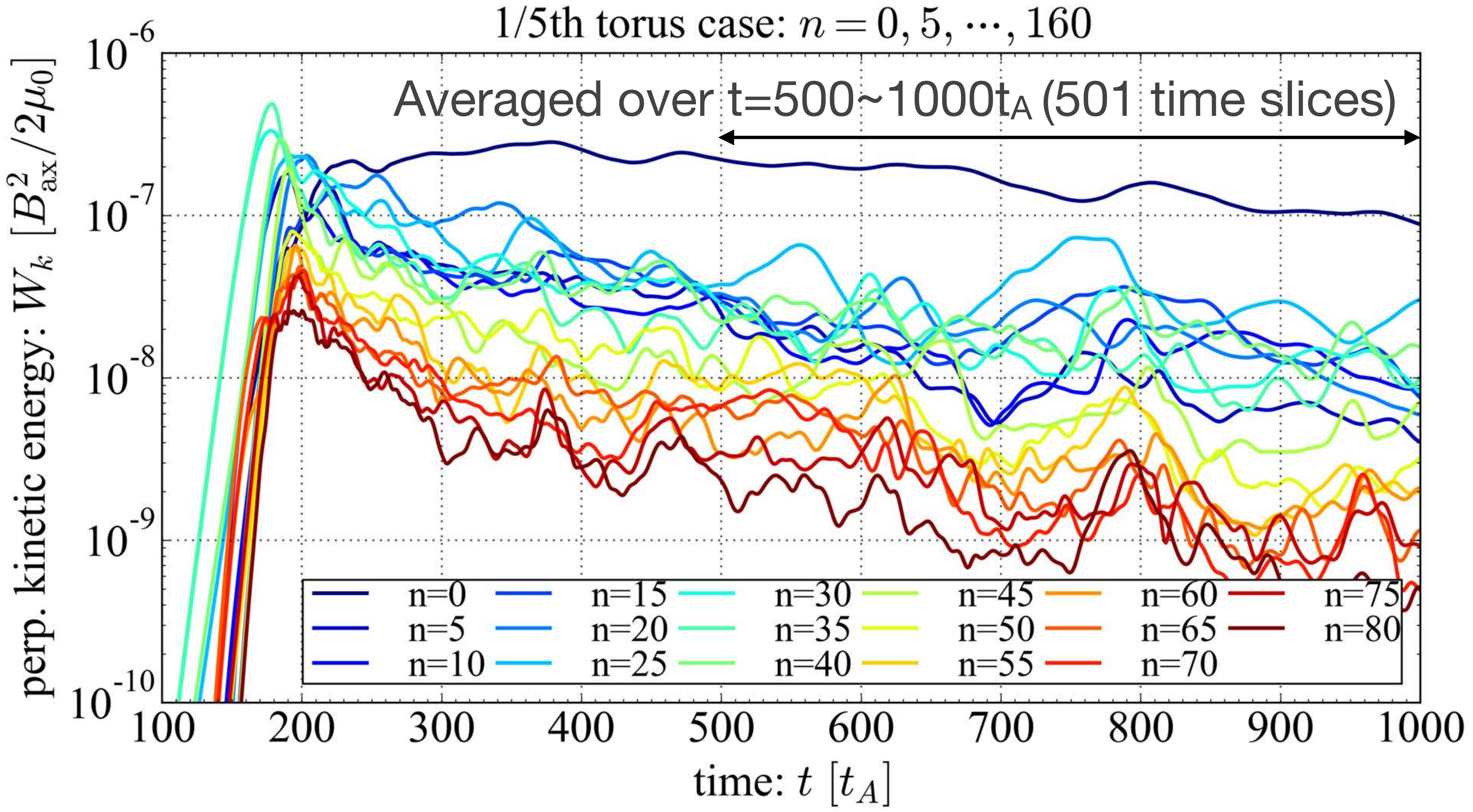

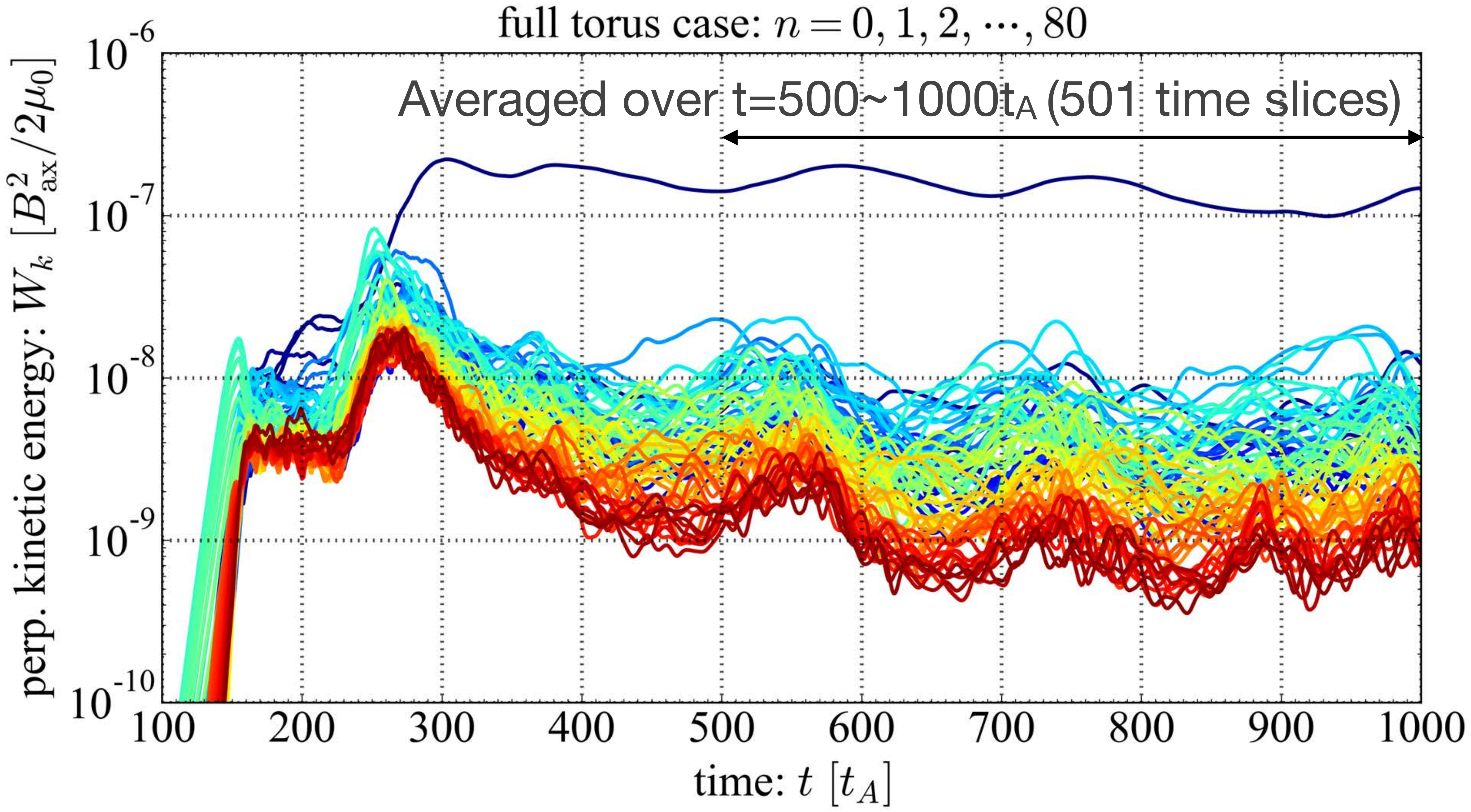

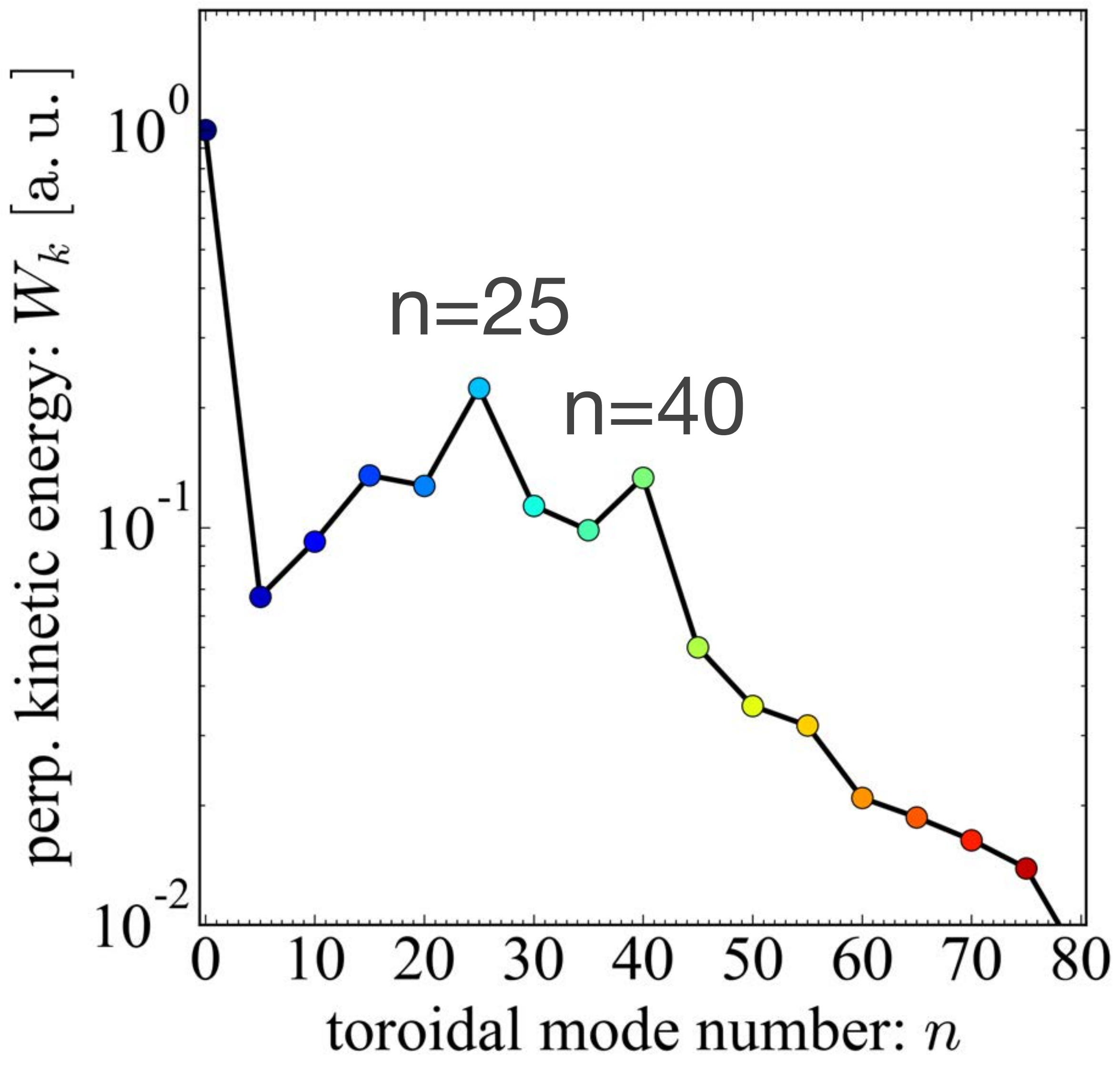

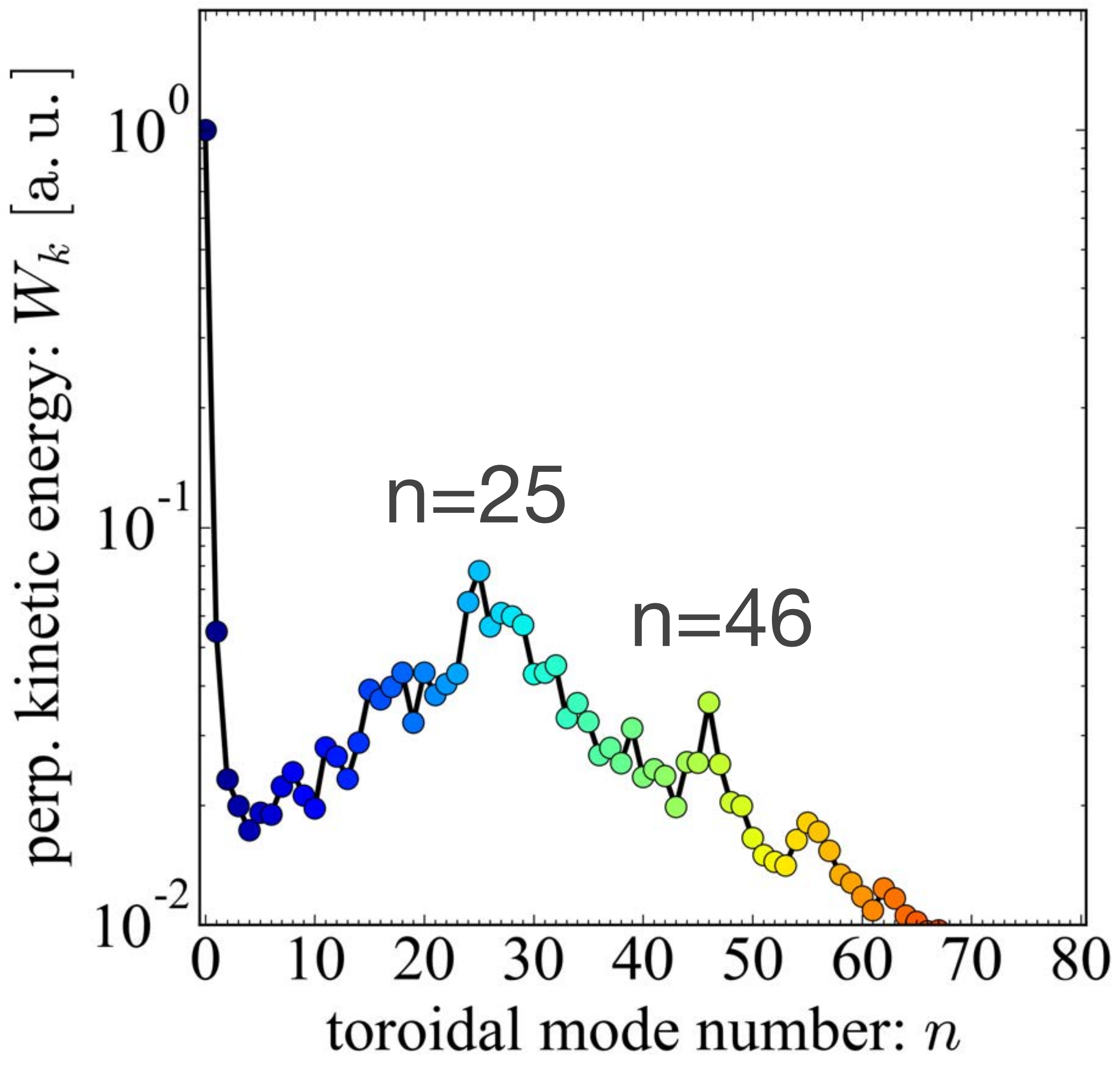

Outline

- Introduction

- Issues on Poisson solvers in BOUT++ and a new Poisson solver developed for low-n modes

- Verification test of 2D Poisson solver by linear problems

- Preliminary pedestal collapse simulation in annular full tours domain in shifted circular geometry

- Summary and future work (research plan in FY2021)

Summary

2D Poisson solver for low-n modes has been developed to extend BOUT++ for tokamak edge simulation solving interplay between n=0, low-n, middle-n and high-n modes in diverted geometries

- Verification test of 2D Poisson solver by linear pressure-driven modes
  - Linear IBM growth rates in circular geometry show good agreement between 2D/1D Poisson solvers
  - Linear RBM growth rates in single-null geometry shows 6~8% difference

  ➡Further tests are required to clarify impact of flute-ordering in complex geometries

- Preliminary pedestal collapse simulation in annular full tours domain in shifted circular geometry
  - Pedestal collapse simulation in full-annular domain using low-n Poisson solver works with acceptable computational cost
  - Introducing low-n modes may change dynamics during pedestal collapse driven by high-n RBM instability but may not change turbulence property after pedestal collapse

  ➡ Production run with high-resolution grid (nx=1024, ny=128, nz=512) is required for further analysis

Future work (research plan in FY2021)

Verification test of 2D Poisson solver by linear problems

- Further ballooning type instability test with ion density profile in diverted geometries
- 2D Poisson solver test with current-driven instabilities (kink/peeling mode) for type-I ELMs

Nonlinear ELM crash simulations

- Pedestal collapse simulation in full-annular diverted geometries
  - ✓ Some nonlinear runs have finished in single-null geometries but further code checks are required
- Simulation of transition from type-I to type-III ELM including resistive ballooning mode (RBM) turbulence in diverted geometry with full toroidal mode spectrum [research target in FY2021]
  - ✓ ELM crashes in a series of ITER like equilibria with different pedestal collisionality
  - ✓ The maximum simulated toroidal mode is scanned to investigate the impact of RBM turbulence on energy loss during pedestal collapses in type-I ELMs, type-III ELMs, and their intermediate regime

    ➡ Maybe useful for understanding dynamics of ELMs in ramp-up/-down phase

flux surface and field-aligned coordinates are employed for tokamak edge sim.

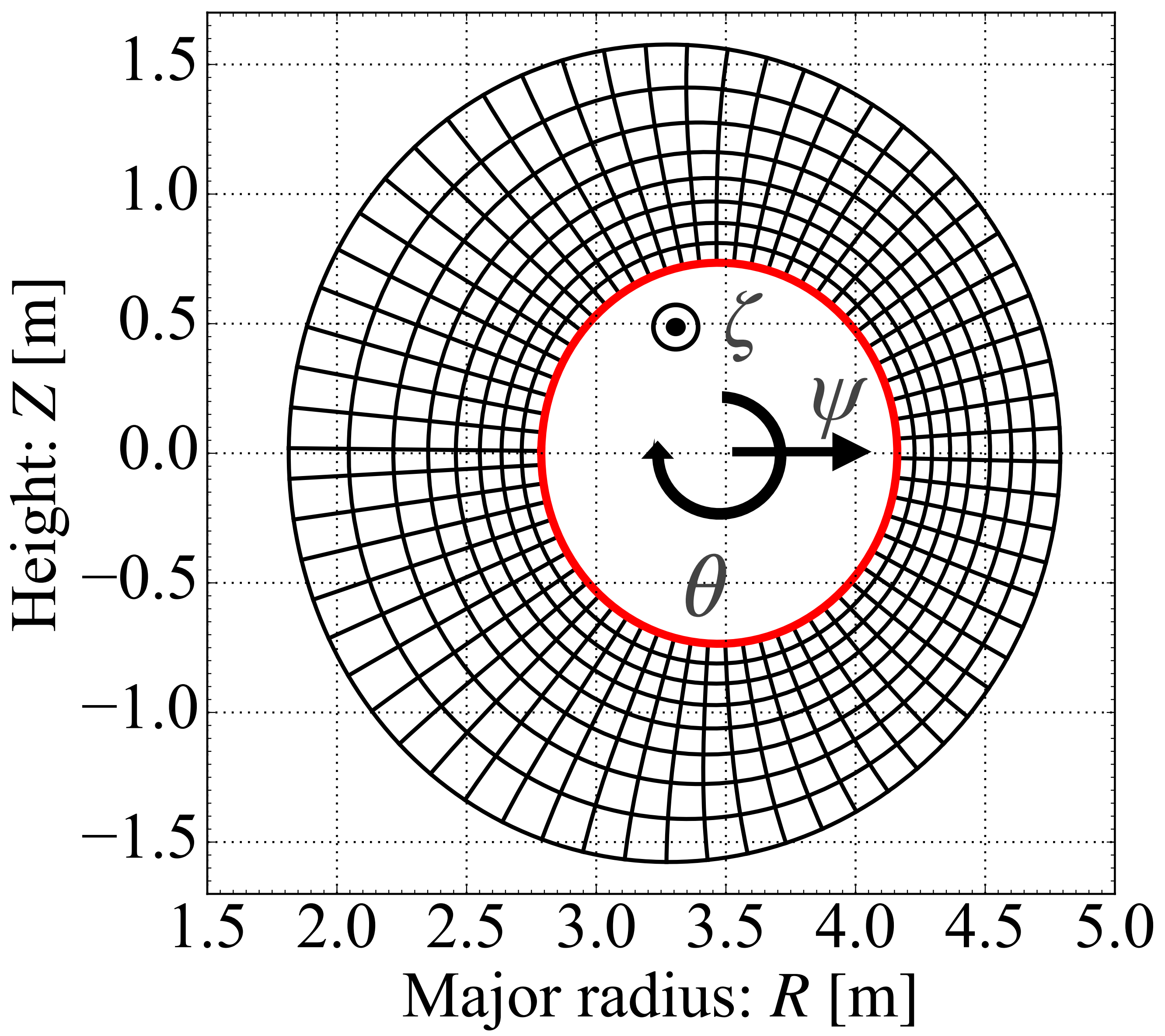

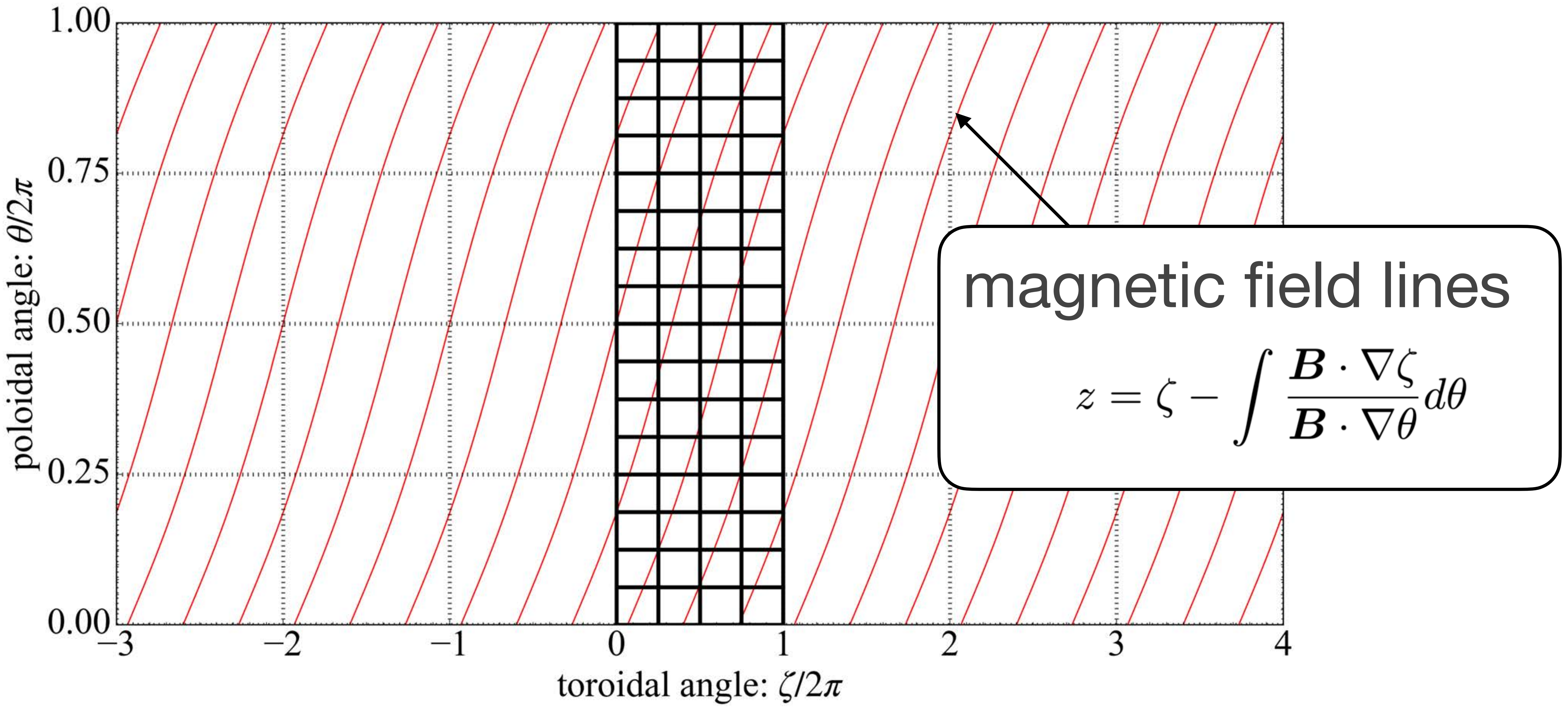

Flux-surface coordinates: (ψ, θ, ζ)

- ψ: poloidal flux function, $[\psi_{in}, \psi_{out}]$
- θ: orthogonal poloidal angle, $[0, 2\pi)$
- ζ: geometrical toroidal angle, $[0, 2\pi/N)$
- periodic boundary condition inside LCFS
  - toroidal: $f(\psi, \theta, \zeta + 2\pi/N) = f(\psi, \theta, \zeta)$
  - poloidal: $f(\psi, \theta + 2\pi, \zeta) = f(\psi, \theta, \zeta)$

Resonant modes have large structures along $\boldsymbol{B}$ but has fine structure perpendicular to $\boldsymbol{B}$

➡A number of poloidal grid is required for resonant poloidal mode m~nq for high-n modes in high-q edge region

flux surface and field-aligned coordinates are employed for tokamak edge sim.

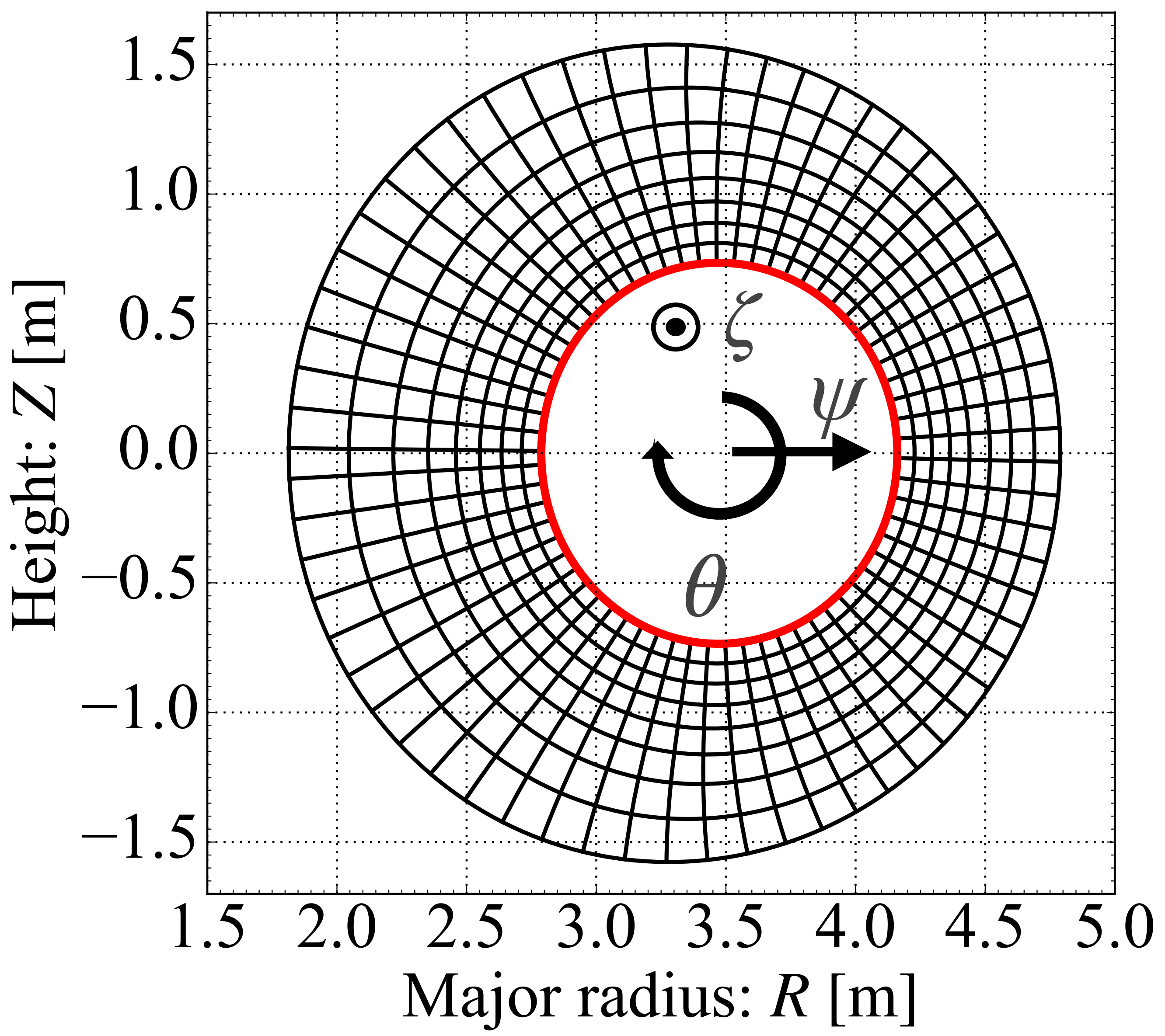

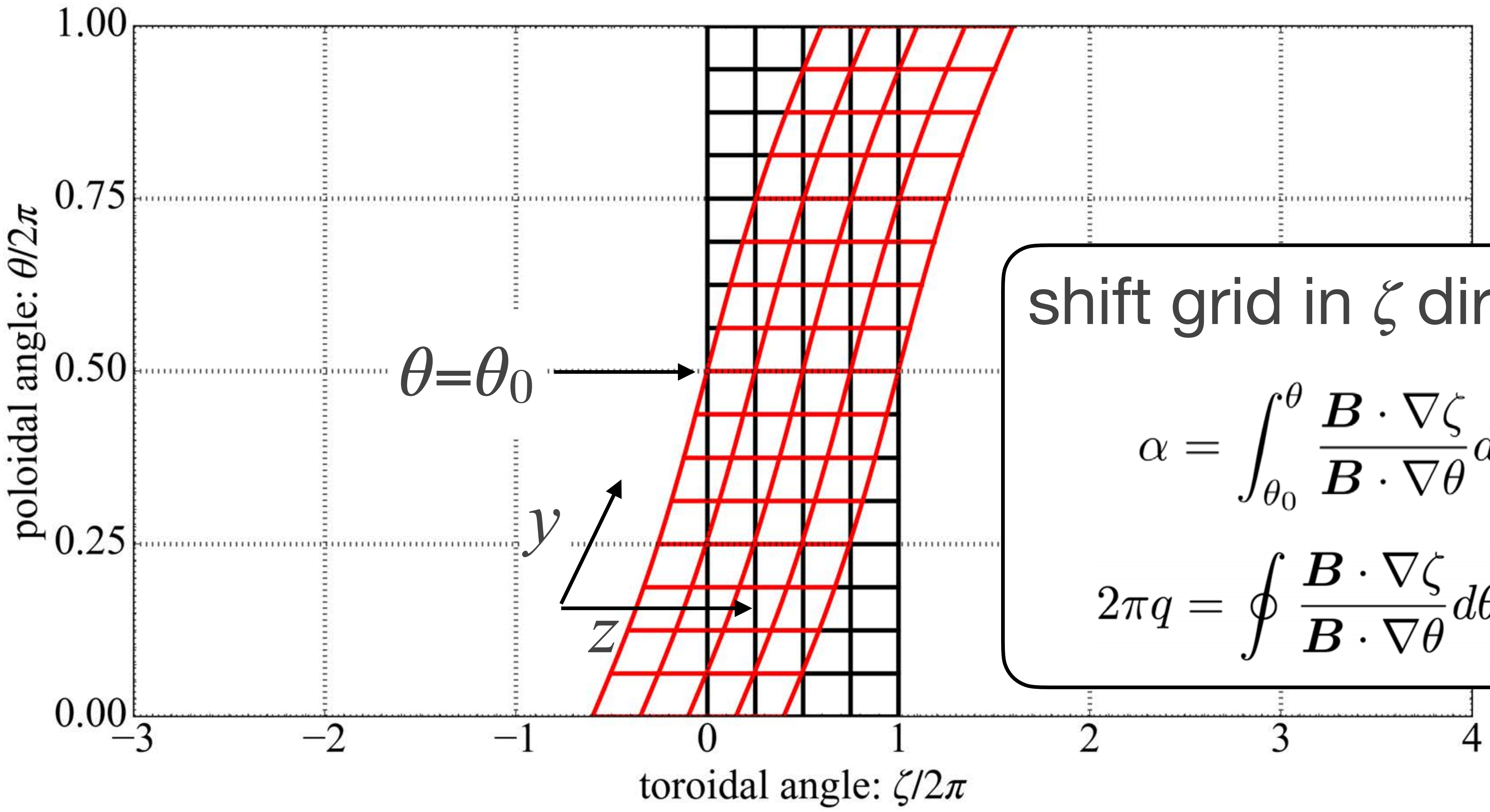

shift grid in ζ direction by α

$$\alpha = \int_{\theta_0}^{\theta} \frac{\boldsymbol{B}\cdot\nabla\zeta}{\boldsymbol{B}\cdot\nabla\theta} d\theta$$

$$2\pi q = \oint \frac{\boldsymbol{B}\cdot\nabla\zeta}{\boldsymbol{B}\cdot\nabla\theta} d\theta$$

Field-aligned coordinates: (x, y, z)

- $x=\psi-\psi_o$: radial label, $[x_{in}, x_{\mathrm{out}}]$
- $y=\theta$: parallel label, $[0,2\pi)$
- $z=\zeta-\alpha$: binormal label, $[0,2\pi/N)$
- periodic boundary condition inside LCFS
  - binormal: $f(x, y, z+2\pi/N) = f(x, y, z)$
  - Parallel: $f(x, y+2\pi, z-2\pi q) = f(x, y, z)$

y-direction is aligned to magnetic field line

➡ Grid points in y-dir. can be reduced significantly

Radial shear of magnetic shear (safety factor) strongly deforms field-aligned grid

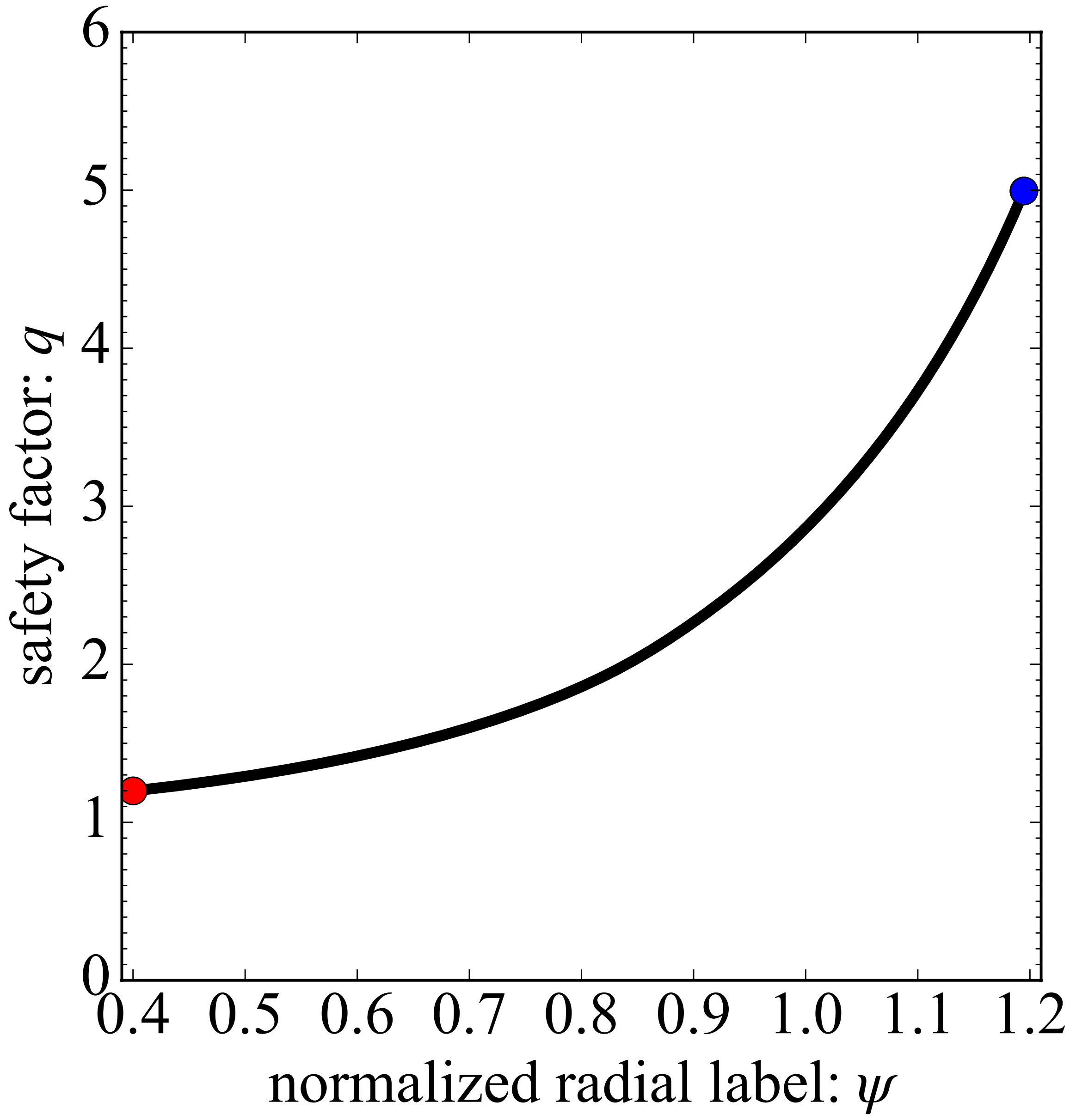

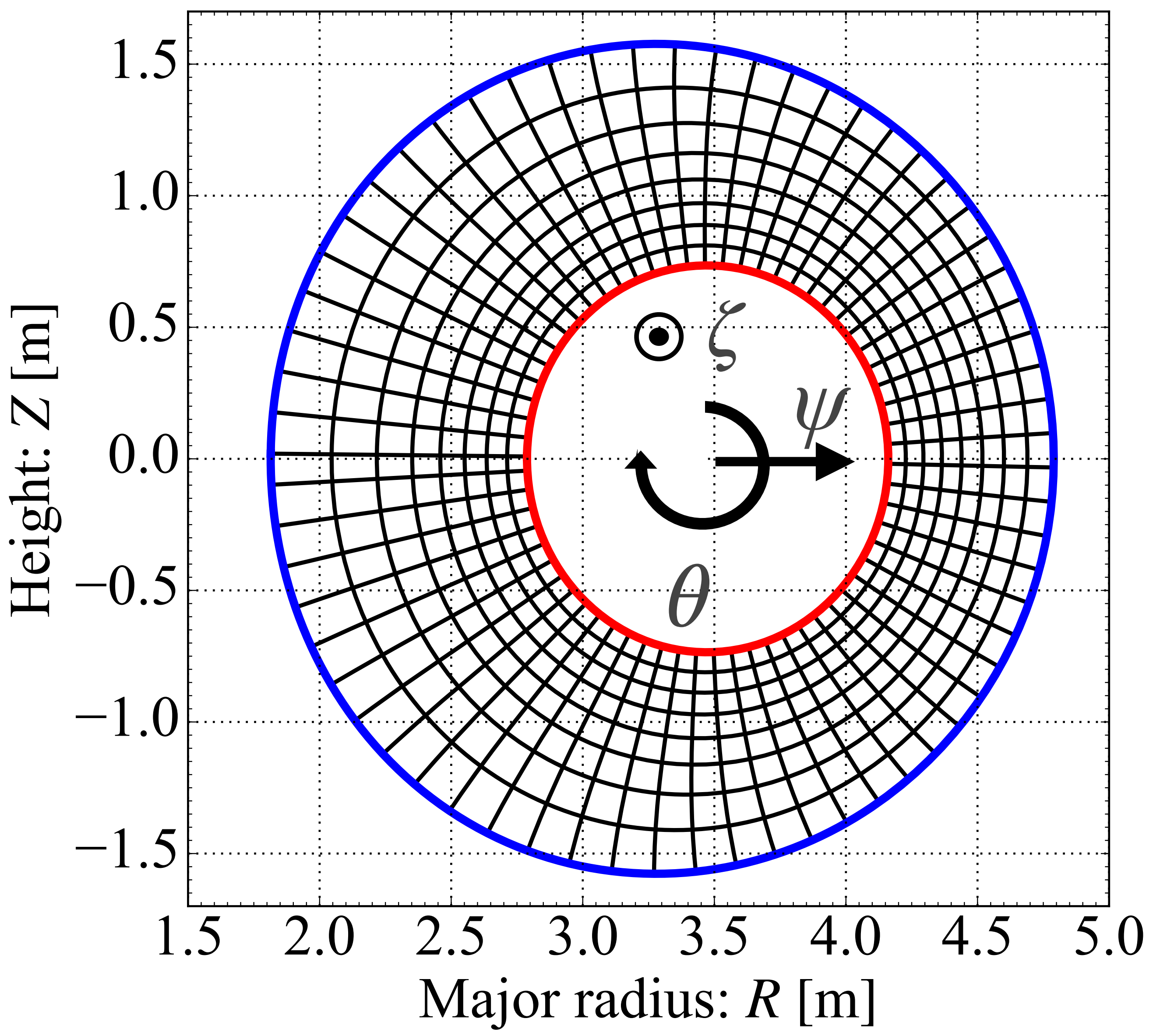

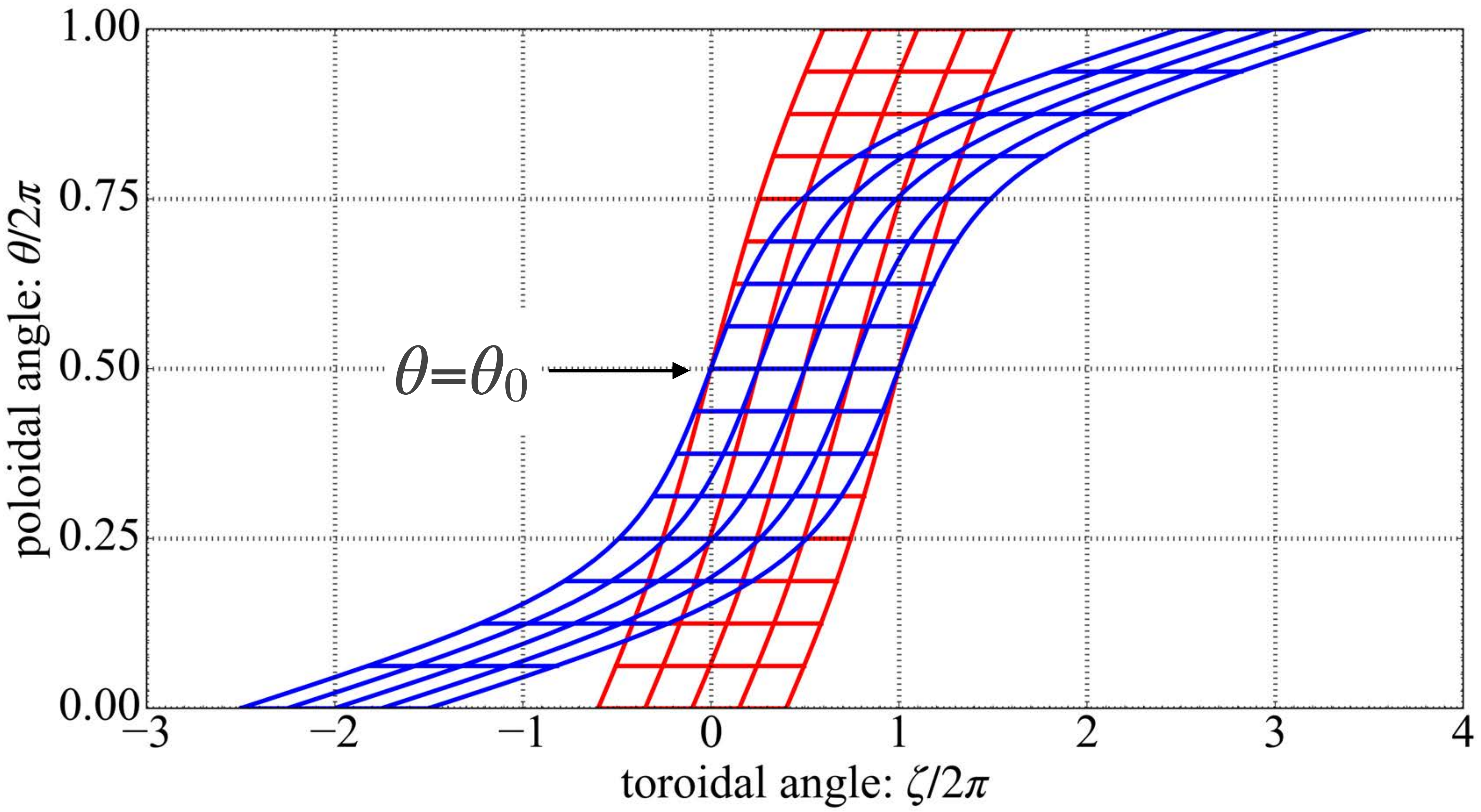

➡Cell deformation strongly degrade accuracy of differencing in radial-direction

Example: cell deformation effect in 1st radial derivative in field-aligned coordinates

$$\frac{\partial}{\partial x} = \frac{\partial}{\partial \psi} + I \frac{\partial}{\partial \zeta}$$

Integrated magnetic shear $I = \int_{\theta_0} \frac{\partial \nu}{\partial \psi} d\theta$

Local magnetic shear $\nu = \frac{\boldsymbol{B} \cdot \nabla \zeta}{\boldsymbol{B} \cdot \nabla \theta}$

Shifted metrics and radial derivatives evaluate spatial differentials accurately

Example: divergence of vector $\boldsymbol{A}$

$$\begin{aligned}\nabla\cdot\boldsymbol{A} =& \frac{1}{J}\frac{\partial}{\partial x}\left(J\boldsymbol{A}\cdot\nabla x\right)+\frac{1}{J}\frac{\partial}{\partial y}\left(J\boldsymbol{A}\cdot\nabla y\right)+\frac{1}{J}\frac{\partial}{\partial z}\left(J\boldsymbol{A}\cdot\nabla z\right)\\ =& \frac{1}{J}\left(\frac{\partial}{\partial\psi}+I\frac{\partial}{\partial z}\right)\left(JA^{\psi}\right)+\frac{1}{J}\frac{\partial}{\partial y}\left(JA^{y}\right)+\frac{1}{J}\frac{\partial}{\partial z}\left(JA^{z'}-IJA^{\psi}\right)\\ =& \frac{1}{J}\frac{\partial}{\partial\psi}\left(JA^{\psi}\right)+\frac{1}{J}\frac{\partial}{\partial y}\left(JA^{y}\right)+\frac{1}{J}\frac{\partial}{\partial z}\left(JA^{z'}\right)\end{aligned}$$

Integrated magnetic shear free form

Reciprocal basis vector of field-aligned coordinates

$$\begin{aligned}\nabla x =& \nabla\psi\\ \nabla y =& \nabla\theta\\ \nabla z =& \nabla\zeta-\nu\nabla\theta-I\nabla\psi\\ J^{-1} =& \nabla x\times\nabla y\cdot\nabla z\\ =& \nabla\psi\times\nabla\theta\cdot\nabla\zeta\end{aligned}$$

- All spatial differences are evaluated in (ψ ,ζ)-plane or (y, z)-plane in integrated magnetic shear free form
  - No mix derivatives with ψ and y due to orthogonality of flux surface coordinates
  - FFT-base coordinate transform for differencing in (ψ ,ζ)-plane

$$f(x,y,z)\xrightarrow{\text{Coord. transform}}f(\psi,\theta,\zeta)\xrightarrow{\text{Differencing}}\frac{\partial f}{\partial\psi}(\psi,\theta,\zeta)\xrightarrow{\text{Coord. transform}}\frac{\partial f}{\partial\psi}(x,y,z)$$